UNIVERSITYᴼF BIRMINGHAM

RhoJ/TCL Regulates Endothelial Motility and Tube Formation and Modulates Actomyosin Contractility and Focal Adhesion Numbers

Kaur, Sukhbir; Leszczynska, Katarzyna; Abraham, S; Scarcia, M; Hiltbrunner, S; Marshall, CJ; Mavria, G; Bicknell, Roy; Heath, Victoria

Link to publication on Research at Birmingham portal

The online version of this article, along with updated information and services, is located on the World Wide Web at:

http://atvb.ahajournals.org/cgi/content/full/31/3/657

Data Supplement (unedited) at:

http://atvb.ahajournals.org/cgi/content/full/ATVBAHA.110.216341/DC1

Subscriptions: Information about subscribing to Arteriosclerosis, Thrombosis, and Vascular Biology is online at
http://atvb.ahajournals.org/subscriptions/

Permissions: Permissions & Rights Desk, Lippincott Williams & Wilkins, a division of Wolters Kluwer Health, 351 West Camden Street, Baltimore, MD 21202-2436. Phone: 410-528-4050. Fax: 410-528-8550. E-mail:
journalpermissions@lww.com

Reprints: Information about reprints can be found online at
http://www.lww.com/reprints

RhoJ/TCL Regulates Endothelial Motility and Tube Formation and Modulates Actomyosin Contractility and Focal Adhesion Numbers

Sukhbir Kaur, Katarzyna Leszczynska, Sabu Abraham, Margherita Scarcia, Sabina Hiltbrunner, Christopher J. Marshall, Georgia Mavria, Roy Bicknell, Victoria L. Heath

Objective—RhoJ/TCL was identified by our group as an endothelial-expressed Rho GTPase. The aim of this study was to determine its tissue distribution, subcellular localization, and function in endothelial migration and tube formation.

Methods and Results—Using in situ hybridization, RhoJ was localized to endothelial cells in a set of normal and cancerous tissues and in the vasculature of mouse embryos; endogenous RhoJ was localized to focal adhesions by immunofluorescence. The proangiogenic factor vascular endothelial growth factor activated RhoJ in endothelial cells. Using either small interfering (si)RNA-mediated knockdown of RhoJ expression or overexpression of constitutively active RhoJ (daRhoJ), RhoJ was found to positively regulate endothelial motility and tubule formation. Downregulating RhoJ expression increased focal adhesions and stress fibers in migrating cells, whereas daRhoJ overexpression resulted in the converse. RhoJ downregulation resulted in increased contraction of a collagen gel and increased phospho–myosin light chain, indicative of increased actomyosin contractility. Pharmacological inhibition of Rho-kinase (which phosphorylates myosin light chain) or nonmuscle myosin II reversed the defective tube formation and migration of RhoJ knockdown cells.

Conclusion—RhoJ is endothelial-expressed in vivo, activated by vascular endothelial growth factor, localizes to focal adhesions, regulates endothelial cell migration and tube formation, and modulates actomyosin contractility and focal adhesion numbers. (*Arterioscler Thromb Vasc Biol*. 2011;31:657-664.)

Key Words: angiogenesis ■ endothelial function ■ Rho GTPase ■ actin cytoskeleton ■ focal adhesion

Endothelial cells line all blood vessels and play a critical role in the formation of new vessels, or angiogenesis. Angiogenesis is involved in physiological processes, such as the female menstrual cycle, but also plays a key role in pathologies, such as diabetic retinopathy and the growth and metastasis of solid tumors.[1] During angiogenesis, endothelial cells perform a variety of functions, including degradation of the extracellular matrix, migration, proliferation, lumen formation, and vessel stabilization,[2] and roles for the Rho GTPases RhoA, Cdc42, and Rac1 have been identified in many of these processes.[3]

Rho GTPases are molecular switches that cycle between active GTP-bound and inactive GDP-bound forms. They were initially identified as regulators of the actin cytoskeleton but have subsequently been shown to be involved in many cellular processes, such as vesicle trafficking, cytokinesis, and gene expression.[4] Actin stress fibers are contractile components of the cytoskeleton that comprise bundles of actin and myosin, known as actomyosin. The small Rho GTPases, RhoA, -B, and -C, when activated, promote stress fiber formation via their activation of Rho-kinase (ROCKI/II,

ROKβ/α); ROCK phosphorylates a number of targets, resulting in increased myosin light chain (MLC) phosphorylation and increased actomyosin contractility.[5] Recently, it was demonstrated that established tubes have greater levels of phospho-MLC and that this is reduced on induction of sprouting.[6] Indeed, inhibition of ROCK or MLC phosphorylation was accompanied by an induction of Rac1-dependent sprouting, suggesting that sprouting angiogenesis is both accompanied by and requires a downregulation of actomyosin contractility.[7] Focal adhesions are large, dynamic protein complexes that mediate connections between the extracellular matrix and the intracellular cytoskeleton. They play a critical role in mechanotransduction, and their coordinated assembly and turnover are required for cell motility.[8]

Using a combination of bioinformatic and expression analyses using reverse transcription and quantitative polymerase chain reaction, our laboratory previously identified the small Rho GTPase RhoJ/TCL (TC10 like) as being highly and specifically expressed by endothelial cells.[9] RhoJ was initially identified by 2 groups as being a novel Rho GTPase related to TC10 (RhoQ),[10,11] belonging to the Cdc42 subfam-

---

ily of Rho GTPases. Cdc42 has a critical role in filopodia formation,[4] whereas TC10 mediates insulin-regulated metabolic events[12]; in contrast, overexpressing constitutively active or inactive forms of RhoJ modulated filamentous (f)-actin formation.[11,13,14] A role for RhoJ in the in vitro differentiation of 3T3 L1 adipocytes has been demonstrated,[15] and, like its close homolog TC10, increased levels of RhoJ-GTP were stimulated by insulin treatment.[10] Subsequent work has shown that epitope-tagged, overexpressed RhoJ localized to early and recycling endosomes, and a role for RhoJ in regulating early endocytosis was identified.[16]

The aim of this study was to further explore the tissue distribution, investigate the activation, and determine the role of RhoJ in endothelial cells. We have identified a vascular expression pattern of RhoJ in both human tissue and mouse embryos and demonstrated that endogenous RhoJ localizes to focal adhesions. We have identified a critical role for this Rho GTPase in mediating endothelial cell motility and tube formation. We also demonstrate that RhoJ plays a role in modulating actomyosin contractility and focal adhesion numbers.

Methods

An expanded Methods section is available in the online Data Supplement at http://atvb.ahajournals.org.

Primary and immortalized cell lines used were human umbilical vein endothelial cells (HUVECs) (passage 1 to 6), human pericytes from placenta (hPC-PL), human aortic smooth muscle cells, HMEC-1 (human microvascular cell line-1), and HEK293T. For small interfering (si)RNA knockdown, HUVECs were transfected with 10 to 25 nmol/L negative control duplex (siControl), RhoJ siRNA duplex 1 (5′-CCACTGTGTTTGACCACTA-3′), or RhoJ siRNA duplex 2 (5′-AGAAACCTCTCACTTACGA-3′). Transfections were performed using either RNAiMAX Lipofectamine (Invitrogen) at a final concentration of 0.3% (vol/vol) or GeneFECTOR (Venn Nova Inc). RNAiMAX was used for all experiments except for the organotypic tube-forming assays and the phospho/total MLC Western blotting. The inhibitors used were Y27632 (10 μmol/L, ROCK inhibitor) or blebbistatin (5 μmol/L, nonmuscle myosin II inhibitor). For lentiviral production the plasmids psPAX2 and pMD2G were used with either pWPXL-GFP-daRhoJ(Q79L) or pWPI (green fluorescent protein [GFP]). GFP-positive HUVECs were sorted before performing assays. Changes in protein expression were assessed by Western blotting.

Scratch wounding of monolayers was achieved using a plastic pipette tip. 2D tube formation was assessed by plating cells on natural Matrigel. In the organotypic tube-forming assay, HUVECs were cocultured with confluent human dermal fibroblasts, and tubule formation was quantified using the AngioSys software.[6,7] Contractility was assessed using cell-mediated contraction of a type I collagen gel.[17] MLC2 phosphorylation was assessed by Western blotting for phospho-MLC2 and total MLC2.[7]

In situ hybridization was performed on human tissue sections, which were costained with digoxigenin-labeled riboprobes/anti-digoxigenin–rhodamine combined with *Ulex europaeus* agglutinin I–fluorescein. The whole-mount in situ hybridization protocol was adapted from Piette et al[18] and performed on embryonic day 9.5 mice using digoxigenin-labeled probes to mouse RhoJ or von Willebrand factor. Immunofluorescence was performed using anti-vinculin, anti–pFAK-Y397, purified rabbit anti-RhoJ antisera, or phalloidin-TRITC and imaged using confocal microscopy. Focal adhesions were manually counted. Levels of actin fluorescence were measured using the LSM 510 confocal software.

Details of experimental repetition are noted in the full and supplemental figure legends in the online Data Supplement; all assays were performed with at least 3 different HUVEC isolates. Data are plotted with error bars representing SEM or are displayed as box and whisker plots: these indicate the maximum, minimum, 25th and 75th percentile, and median values. To test statistical differences in defined pairs of groups, the Mann–Whitney test was performed except for the scratch-wound and gel-contraction assays, where the Student t test was used. Statistical significance is denoted as follows: ***$P<0.001$, **$P=0.001$ to 0.01, and *$P=0.01$ to 0.05.

Results

RhoJ Is Expressed in Endothelial Cells

RhoJ expression was localized by in situ hybridization both on human tissue sections and in the developing mouse embryo. *U europaeus* agglutinin I was used as a marker of endothelium, because it recognizes an endothelial specific glycosylation,[19] and this colocalized with RhoJ in endothelial cells lining vessels in a number of adult human tissues (heart, adrenal gland, lymph node, muscle, pancreas, placenta, liver, lung, bladder cancer, bone cancer, and ovarian cancer). However, expression was not found in the vessels of testis, brain, kidney, stomach, colon, or rectal cancer (Figure 1A and supplemental Figure I in the online Data Supplement). The RhoJ probe also stained some nonendothelial cells, including muscle, liver, and some cancer cells, suggesting that RhoJ expression is not restricted to the endothelium. Because this vessel-like expression pattern may be attributable to expression of RhoJ by nonendothelial vessel cell types, its expression was tested in human placental-derived pericytes and aortic smooth muscles cells. Low levels of RhoJ message and protein were found in isolates of both cell types at a level much lower than that seen in endothelial cells (supplemental Figure II).

Whole-mount in situ hybridization was performed at embryonic day 9.5, the stage at which the vasculature is developing and angiogenesis is occurring in the developing mouse.[20] RhoJ, like the endothelial expressed gene von Willebrand factor,[21] is expressed in the main trunk vessels and intersomitic vessels (Figure 1B). These data are consistent with an endothelial expression pattern of RhoJ in developing vessels.

To determine the intracellular localization of endogenous RhoJ, purified rabbit polyclonal antiserum was developed and validated using RhoJ knockdown in HUVECs or RhoJ overexpression in a nonendothelial cell type (data not shown). Using this reagent, RhoJ was localized in punctuate regions of the cell, and costaining with anti-vinculin antibodies or anti-phospho(397) FAK antibodies indicated that these structures were focal adhesions (Figure 1C). Because RhoJ is closely related in structure and amino acid sequence to other members of the Rho GTPase family, we established that neither this RhoJ polyclonal antisera nor the RhoJ monoclonal antibodies used in this study for Western blotting recognized Cdc42, Rac1, or RhoA (supplemental Figure III).

RhoJ Plays a Role in Endothelial Cell Motility, Growth, and Tube Formation

To determine whether RhoJ plays any role in endothelial cell biology and angiogenesis, a series of assays were performed using HUVECs with either siRNA-mediated knockdown of RhoJ or overexpression of dominant-active RhoJ. Knockdown of RhoJ protein was performed using 2 RhoJ-specific duplexes (RhoJ D1 and RhoJ D2); as a control, cells were either mock-transfected or transfected with a negative control duplex (siControl). Angiogenesis requires both endothelial
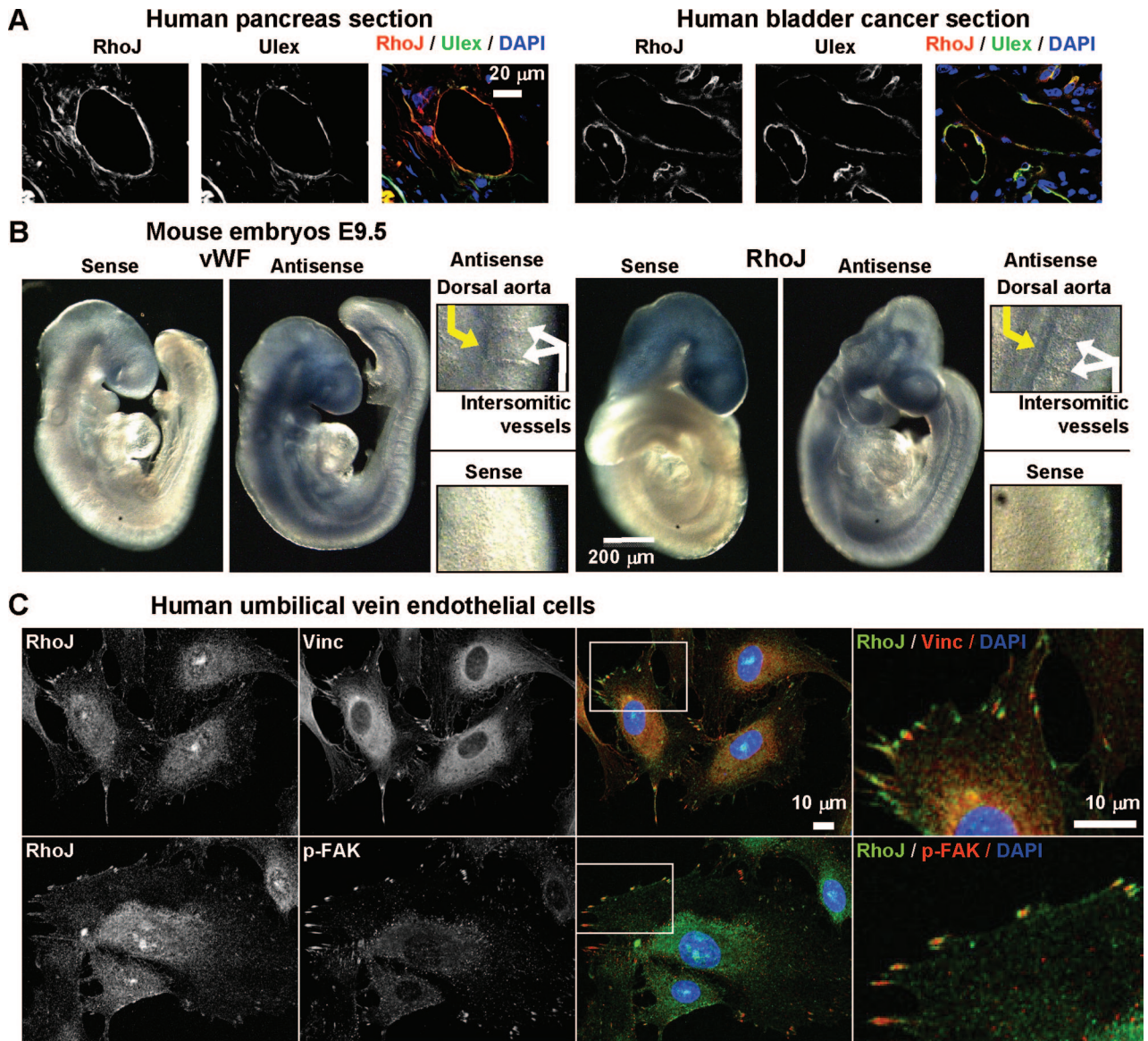
Figure 1. RhoJ expression patterns. A, In situ hybridization of RhoJ in combination with *U europaeus* agglutinin I (endothelial cells) in human tissue sections. B, In situ hybridization of RhoJ and von Willebrand factor (vWF) (endothelial marker) in mouse embryos. C, Immunofluorescence of RhoJ with anti-vinculin or anti-phospho (Y397) FAK. Detailed figure legends are included in the online Data Supplement.

cell motility and proliferation. Chemokinetic motility was assessed using a basic scratch-wound assay. A scratch was made in a monolayer of HUVECs 2 days after transfection. Unlike the control cells (mock and siControl), cells with reduced RhoJ expression (RhoJ D1 and D2) did not migrate to close the scratch; at 24 hours, there was still a region of scratch evident (Figure 2A). The mean area of scratch remaining at different time points was quantified from 3 independent experiments (Figure 2C), and statistically significant differences observed at 24 hours by comparing either of the RhoJ siRNA duplex–treated groups with the siScramble control. Mitomycin C was added to this assay to prevent cell division, strongly suggesting that it is impaired cell motility in the RhoJ knockdown cells, rather than a proliferative defect, that prevented closure. The RhoJ knockdown efficiently knocked down RhoJ protein levels (Figure 2E) but did not alter the levels of Cdc42, Rac1, or RhoA in endothelial

cells (supplemental Figure IV). The absence of any interferon response at duplex concentrations used for any of the various assays was confirmed by monitoring expression of the interferon inducible genes 2′,5′-oligoadenylate synthetase 1[22] and IFN-stimulated gene of 20 kDa[23] (data not shown).

The effect of expressing a GFP-tagged dominant active Q79L mutant of RhoJ,[11] permanently in the GTP-bound active form, was also assessed. HUVECs were transduced with lentivirus to express either GFP or GFP-daRhoJ; GFP-expressing cells were then purified by cell sorting; expression of the GFP or GFP-daRhoJ was confirmed by Western blotting (Figure 2F and supplemental Figure VA). GFP-daRhoJ primarily localized to the plasma membrane, where it was more concentrated in focal adhesions, there was also some localization to intracellular vesicles (supplemental Figure VB). By contrast to the siRNA knockdown, the overexpression of GFP-daRhoJ slightly but reproducibly accelerated wound closure in at least 3
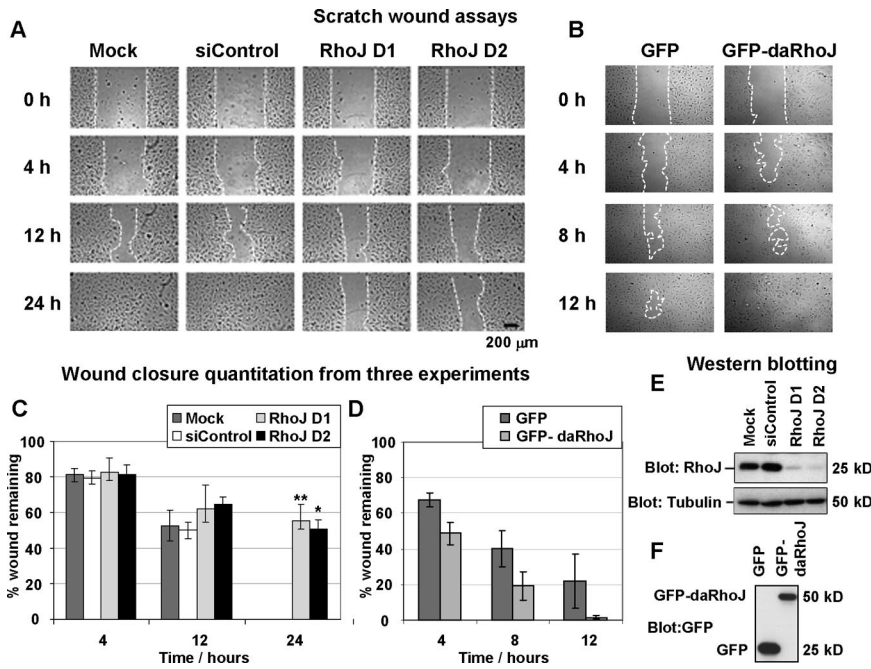
Figure 2. RhoJ regulates endothelial cell motility. HUVECs were transfected with siControl or RhoJ siRNA duplexes or were mock-transfected (concentration: 10 nmol/L) (A, C, and E) or lentivirally transduced to express GFP or GFP-daRhoJ (B, D, and F). Scratch-wound assays were performed (A and B), closure was quantified (C and D), and Western blots were performed to show RhoJ knockdown (E) or ectopic GFP/GFP-daRhoJ expression (F).

experiments (Figure 2B and 2D). However, variations in the speed of wound closure between different HUVEC isolates meant that significant differences are not revealed by performing statistical tests on the combined data at different time points. These data strongly suggest a role for RhoJ in mediating endothelial cell movement.

The effect of RhoJ knockdown on endothelial cell proliferation and chemotaxis was also assessed; there was slightly reduced cell growth in RhoJ D1– or RhoJ D2–transfected endothelial cells compared with mock- or siControl-transfected cells (supplemental Figure VIA). This diminished proliferation was not associated with any changes in the cell cycle distribution, but small increases in the level of apoptosis were observed (supplemental Figure VIB). Knockdown of RhoJ also inhibited chemotaxis through the porous filters in response to chemoattractant, again suggesting a role for RhoJ in endothelial cell motility (supplemental Figure VIC).

Finally, endothelial tube formation was assessed both using a Matrigel tube-forming assay and an organotypic angiogenesis assay. HUVECs transfected with RhoJ-specific siRNA duplexes produced a more poorly connected network of cells when plated on Matrigel, a solubilized basement membrane extract, compared with the control-transfected cells. These networks were less stable, with more cell retraction observed at 24 hours (supplemental Figure VII).

In the organotypic assay, HUVECs are cocultured with human dermal fibroblasts. The interaction of these cell types results in the formation of endothelial derived tubules with lumens that are embedded in naturally produced extracellular matrix.[24] This process is entirely dependent on the 2 major angiogenic factors: basic fibroblast growth factor, present in the culture media; and vascular endothelial growth factor (VEGF), produced by the fibroblasts; and the resulting tubules are highly reminiscent of capillaries formed during angiogenesis in vivo.[25,26] HUVECs were either mock-transfected or transfected with control or RhoJ-specific

siRNA duplexes and seeded on to a confluent monolayer of human dermal fibroblasts, and tubules were allowed to develop for 5 days. Knockdown of RhoJ resulted in highly impaired tube formation in this assay, with there being significantly fewer, shorter, and lesser-branched tubes (Figure 3A and 3B). Knockdown of RhoJ was assessed by Western blotting at later time points, transfection with RhoJ D1 and D2 at 20 nmol/L gave a knockdown of approximately 60% and 40%, respectively, after 4 days (supplemental Figure VIII).

In contrast, HUVECs overexpressing GFP-daRhoJ produced a greater number of highly branched tubules with a shorter mean length (Figure 3C and 3D). These data indicate a role for RhoJ in tubule formation in these assays. siRNA-mediated knockdown of RhoJ in the human microvascular cell line HMEC-1 (human microvascular cell line-1) also resulted in impaired scratch-wound closure (supplemental Figure IX) and tube formation on Matrigel (supplemental Figure X).

Because tube formation is VEGF-dependent in the coculture assay,[26] and VEGF is one of the most potent proangiogenic factors, assays were performed to assess whether RhoJ is activated by VEGF. HUVECs were treated with VEGF, and levels of both active RhoJ and Cdc42 were determined by pull down of the active GTP-bound forms of these proteins with a glutathione S-transferase fusion of the PAK1 CRIB domain and Western blotting. Densitometry was performed and levels of active Cdc42 and RhoJ in pull-downs versus cellular lysates were determined. Activation of Cdc42 peaked at 15 minutes, and its activity declined thereafter, a result consistent with previous reports.[27] RhoJ, like Cdc42, was activated by VEGF, but its level of activation was more modest, with a slower and more sustained induction (supplemental Figure XI).

RhoJ Modulates Actomyosin Contractility, Actin Stress Fibers, and Focal Adhesions
The data thus far have implicated a critical role for RhoJ in regulating endothelial cell motility, and because Rho GTPases
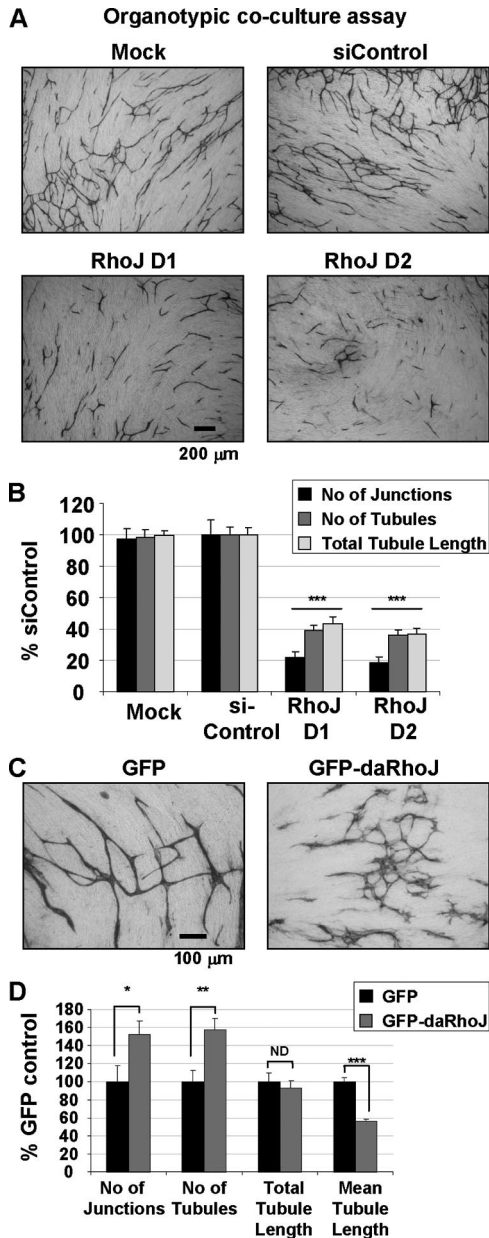
A Organotypic co-culture assay

B

C

D

Figure 3. RhoJ regulates tubule formation. HUVECs were transfected with siControl or RhoJ siRNA duplexes or were mock-transfected (concentration: 20 nmol/L) (A and B) or lentivirally transduced to express GFP or GFP-daRhoJ (C and D). HUVECs were plated on confluent human dermal fibroblasts (HDF) and after 7 days tubules were stained (A and C). Tubule number, length, and number of junctions were quantified (B and D).

A Vinculin immunofluorescensce at the wound edge

B

Figure 4. RhoJ activity affects focal adhesion number in migrating cells. A, HUVECs were mock-transfected, transfected with siControl or RhoJ siRNA duplexes (concentration:10 nmol/L), or lentivirally transduced to express GFP or GFP-daRhoJ; scratch-wound assays and immunofluorescence using anti-vinculin antibodies were performed. B, Focal adhesion quantification in cells at the wound edge.

have been shown to control the actin cytoskeleton and RhoJ localizes to focal adhesions, experiments were performed to investigate how RhoJ knockdown might affect both f-actin and focal adhesion formation.

In initial experiments, HUVECs were either mock-transfected or transfected with siControl, RhoJ D1, or D2, and after 2 days, cells were adhered to gelatin-coated coverslips at a low density and were stained with phalloidin to detect f-actin and with anti-vinculin antibodies to visualize focal adhesions. The control-transfected HUVECs generally showed a modest number of stress fibers and focal adhesions, and the cells had a number of cellular extensions (supplemental Figure XIIA). In

contrast, cells with reduced RhoJ expression had a more circular appearance with fewer cell protrusions and increased numbers of stress fibers, which, in many cells, were observed around the cell edge. Knockdown of RhoJ also resulted in significantly more numerous focal adhesions (supplemental Figure XIIB).

Endothelial cells in vessels are normally found as a monolayer surrounded by other endothelial cells; the exceptions to this are the endothelial tip cells found at the leading end of an angiogenic sprout.[28] To assess whether RhoJ knockdown differentially affected f-actin and focal adhesion numbers in endothelial cells depending on their cellular context, cells at the edge of a scratch wound at the migration front were compared with those found within a monolayer. Two days after transfection, a scratch was made, and the cells were allowed to migrate before they were fixed and stained with either fluorescently conjugated phalloidin or anti-vinculin antibodies. siRNA-mediated knockdown of RhoJ resulted in significantly increased focal adhesion numbers in cells at the edge of a scratch compared with control-transfected cells (Figure 4A and 4B); in contrast, no differences were observed in cells within the monolayer (data not shown).

Figure 5. RhoJ influences stress fibers and actomyosin contractility. HUVECs were transfected with siControl, RhoJ siRNA duplexes or mock-transfected (concentration: 10 nmol/L) (A, B, E, and F) or lentivirally transduced to express GFP or GFP-daRhoJ (C through E), scratch-wound assays were performed, and f-actin was visualized (A and C) and quantified (B and D). Contractility was measured by collagen gel contraction (E) or phospho- and total MLC blotting (F).
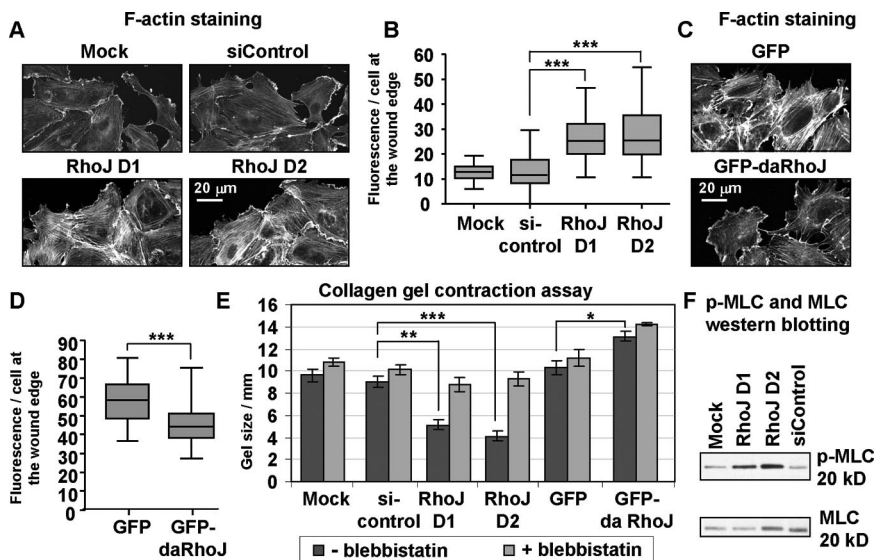
RhoJ knockdown did not affect the localization of VE-cadherin at the cell junctions within the monolayer, suggesting that cell–cell adhesion is not affected. Lentiviral transduction of HUVECs with GFP-daRhoJ resulted in slightly faster wound closure, and enumeration of focal adhesion numbers showed that overexpression of GFP-daRhoJ resulted in cells at the wound edge with significantly fewer focal adhesions than the GFP controls (Figure 4A and 4B). Again no differences were observed in the monolayer. These data indicate a role for RhoJ in regulating focal adhesion disassembly or turnover.

Similarly, using phalloidin staining of both RhoJ siRNA–treated HUVECs and HUVECs overexpressing GFP-daRhoJ, f-actin in cells at the wound edge and in the monolayer was examined. Whereas no differences were observed in cells in the monolayer (data not shown), knocking down RhoJ expression was found to increase the numbers of stress fibers in cells at the wound edge (Figure 5A). This was quantified by measuring fluorescence levels in each cell, and significant increases were found in cells treated with either of the RhoJ-specific duplexes compared with the controls (Figure 5B). Expression of GFP-daRhoJ had the opposite effect, significantly reducing levels of stress fiber in cells at the migration front (Figure 5C and 5D). Thus, RhoJ may play a role in negatively regulating stress fibers formation in migrating cells.

The increased actin stress fiber formation may reflect increased actomyosin contractility. Recently, it has been demonstrated that quiescent tubes have an increased contractility compared with sprouting tubes, and, indeed, a reduction in contractility was required to enable endothelial cell sprouting.[7] The effect of RhoJ in regulating contractility was measured in 2 ways: by measuring endothelial cell–mediated contraction of a type I collagen gel and by determining the levels of phospho-MLC in endothelial cells forming tubes on Matrigel.

An assay previously used to measure endothelial contractility and traction was performed[17]; siRNA-transfected HUVECs or HUVECs expressing GFP/GFP-daRhoJ were imbedded in a collagen gel. After 2 days, the gels were released from the sides of the well, and the plates were incubated for a further 5 days, as the contractility developed within the cells, so the gel retracted, and the amount of contractility was assessed by measuring the diameter of the gel. As a control, 5 μmol/L blebbistatin, an inhibitor of nonmuscle myosin II,[29] was added. Knockdown of RhoJ expression with either of the RhoJ-specific duplexes resulted in a highly significant increase in contraction, which was mostly reversed with blebbistatin. GFP-daRhoJ expression resulted in a small but significant reduction in the contractility compared with cells expressing GFP alone (Figure 5E). Knockdown of RhoJ was also associated with increased phospho-MLC in HUVECs plated on Matrigel, indicating that these cells have increased actomyosin contractility (Figure 5F). No differences were seen in the levels of phospho-MLC as a result of expressing GFP-daRhoJ.

Collectively, these data suggest that RhoJ may be involved in promoting endothelial cell motility and tube formation by negatively regulating MLC phosphorylation and reducing actomyosin contractility. In this case, pharmacological inhibition of ROCK, a kinase that catalyzes MLC phosphorylation,[5] should reverse the impaired motility and tube formation induced by RhoJ knockdown. Indeed, we found that the ROCK inhibitor Y27632, when added to RhoJ siRNA–treated endothelial cells, restored motility both in the scratch-wound assay (Figure 6A and 6B) and Boyden chamber chemotaxis assay (supplemental Figure XIII). RhoJ knockdown cells migrated to close the scratch when treated with the ROCK inhibitor at a similar rate to that of the negative control duplex treated cells (Figure 6A and 6B). Additionally, ROCK inhibition restored the impaired tube formation on Matrigel of RhoJ siRNA–transfected cells, resulting in a more connected and stable tube formation, equivalent to that seen in the negative control duplex–treated cells (Figure 6C and 6D). Addition of 10 μmol/L ROCK inhibitor Y27632 resulted in reduction in phospho-MLC in all samples (supplemental Figure XIV). Similar data were obtained with a structurally unrelated ROCK inhibitor H1152, with the other RhoJ siRNA duplex D1 (data not shown) and with 5 μmol/L blebbistatin, a myosin II inhibitor (supplemental Figures XV and XVI). These data strongly suggest that RhoJ is a negative regulator of actomyosin contractility.
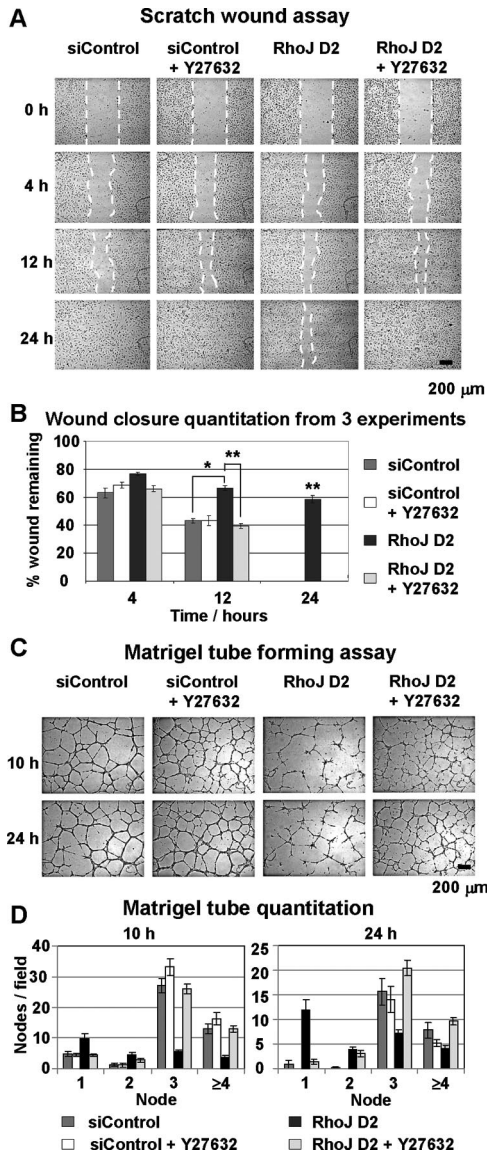
A   Scratch wound assay

B   Wound closure quantitation from 3 experiments

C   Matrigel tube forming assay

D   Matrigel tube quantitation

Figure 6. Inhibition of ROCK restores migration and tube formation in RhoJ siRNA–treated HUVECs: scratch-wound (A) and Matrigel (C) assays were set up 2 days after transfection with siControl or RhoJ D2 (concentration: 10 nmol/L), with or without addition of ROCK kinase inhibitor Y27632. These assays were quantified (B and D).

Discussion

These data are the first to determine the intracellular localization of RhoJ, demonstrate endothelial expression in tissues, show activation by VEGF, and identify a pivotal role for this Rho GTPase RhoJ in endothelial cell motility, tube formation, and modulation of the actin cytoskeleton and focal adhesion formation.

Previous bioinformatic and primary cell line expression studies performed by our laboratory identified RhoJ as having an endothelial specific mRNA expression pattern.[9] In this present study, we have demonstrated expression by endothelial cells in vessels in a number of tissues and cancer types, although it is absent from brain vessels and from normal and cancerous tissue of the digestive tract. We also demonstrate a vascular expression pattern of RhoJ in the mouse embryo, at

a stage in development when angiogenesis is occurring. This expression pattern suggests that it plays a role in the normal functioning of endothelial cells in a number of tissues, as well as potentially in angiogenesis. Although expression levels of RhoJ are high in endothelial cells, we have observed low levels of expression in nonendothelial cell types, indicating that expression of RhoJ is not restricted to endothelial cells.

The function of RhoJ in endothelial cells was probed by using both siRNA-mediated knockdown of RhoJ expression and expression of a constitutively active form of RhoJ, locked into its GTP-bound form. As expected, these 2 approaches gave contrasting phenotypes. Knockdown of RhoJ resulted in impaired migration and tube formation, whereas daRhoJ promoted motility and excessive sprouting during tube formation. Knocking down RhoJ expression using siRNA duplexes impaired cell migration and reduced proliferation, processes involved at early time points in the formation of tubules in the organotypic model. In addition, the RhoJ siRNA–induced increased contractility would have also been likely to be detrimental to tube formation, because previously increased actomyosin contractility resulted in cell detachment and cell death in this model of tubule formation.[6] In contrast, the chaotic appearance of the tubules observed with the daRhoJ is reminiscent of abnormal, sprouting endothelium, a process dependent on VEGF receptor 2.[30] The use of the organotypic assay enabled the identification of a role for RhoJ in tubulogenesis in a physiological setting; however, we are unable to conclude downstream of which soluble or extracellular matrix factor RhoJ is acting in this system. Knocking down RhoJ did not affect the expression of the other major Rho GTPases, RhoA, Rac1, or Cdc42, and we conclude that RhoJ is playing a distinct role in endothelial cells.

To understand the molecular mechanisms by which RhoJ was acting, the effect of modulating its activity on focal adhesions numbers and contractility was investigated. Reducing the activity of RhoJ resulted in increased numbers of focal adhesion and stress fibers in cells migrating at the edge of scratch; additionally, we observed an increase in the physical contractility, as measured by the contraction of a collagen gel. Expressing daRhoJ again gave the converse phenotype. Interestingly, the stress fiber and focal adhesion phenotype was only evident in migrating cells, either plated sparsely or at a scratch-wound edge, and not in cells within a monolayer. This suggests that RhoJ plays a critical role in migrating cells, whereas in cells within a monolayer, the effects of modulating RhoJ expression may be inhibited through signaling from neighboring cells. This lack of phenotype observed in the monolayer may explain why siRNA-mediated downregulation of RhoJ did not inhibit early wound closure (Figure 2A and 2C), with the accumulation of focal adhesions and f-actin occurring only after the cells had started to move and had reduced contact with neighboring cells.

We have additionally demonstrated that RhoJ knockdown results in an increase in MLC phosphorylation. MLC can be phosphorylated by a number of kinases including RhoA-dependent ROCK and Ca^{2+}-dependent MLC kinase, which result in increased myosin ATPase activity and increased stress fiber contractility.[31] Using 2 structurally unrelated inhibitors of ROCK or an inhibitor of nonmuscle myosin II,

the motility defect of RhoJ siRNA–treated endothelial cells was reversed in both the scratch-wound and Matrigel tube-forming assays. There is evidence that reduced contractility is required for endothelial sprouting to occur,[6,7] and our data suggest that RhoJ may play a role in this process.

At present, we do not know the molecular basis by which RhoJ affects contractility and focal adhesion numbers. There is a complex interplay and reciprocal regulation between focal adhesion maturation, turnover, and actomyosin contractility; thus, components of focal adhesions have been shown to regulate contractility, and, conversely, modulating myosin II activity can influence focal adhesion size and distribution.[32] Thus, RhoJ may regulate actomyosin contractility via dynamic regulation of focal adhesions.

This hypothesis is consistent with the localization of endogenously expressed RhoJ to focal adhesions. Previously, only localization of overexpressed RhoJ to early and recycling endosomes had been reported,[16] and, indeed, we have observed the same. Because overexpressing proteins can often drive aberrant localization, we developed a purified polyclonal antiserum that, unlike the commercially available anti-RhoJ monoclonal antibodies, recognized endogenous RhoJ. Because a role for RhoJ in early endocytic recycling has been reported, we investigated whether RhoJ knockdown affected surface levels of VEGF receptor 2 either in resting cells or after VEGF stimulation; in neither case were any differences noted (data not shown).

In conclusion, we have identified RhoJ as a new player in endothelial cell biology. We have demonstrated that this endothelial-expressed Rho GTPase is activated by VEGF and is able to modulate actomyosin contractility and focal adhesion assembly. It plays a critical role in endothelial cell motility and tube formation and will likely prove to be a key player in angiogenesis in vivo.

Disclosures

None.

References

1. Heath VL, Bicknell R. Anticancer strategies involving the vasculature. *Nat Rev Clin Oncol*. 2009;6:395–404.
2. Adams RH, Alitalo K. Molecular regulation of angiogenesis and lymphangiogenesis. *Nat Rev Mol Cell Biol*. 2007;8:464–478.
3. Bryan BA, D'Amore PA. What tangled webs they weave: Rho-GTPase control of angiogenesis. *Cell Mol Life Sci*. 2007;64:2053–2065.
4. Burridge K, Wennerberg K. Rho and Rac take center stage. *Cell*. 2004;116:167–179.
5. Riento K, Ridley AJ. Rocks: multifunctional kinases in cell behaviour. *Nat Rev Mol Cell Biol*. 2003;4:446–456.
6. Mavria G, Vercoulen Y, Yeo M, Paterson H, Karasarides M, Marais R, Bird D, Marshall CJ. ERK-MAPK signaling opposes Rho-kinase to promote endothelial cell survival and sprouting during angiogenesis. *Cancer Cell*. 2006;9:33–44.
7. Abraham S, Yeo M, Montero-Balaguer M, Paterson H, Dejana E, Marshall CJ, Mavria G. VE-Cadherin-mediated cell-cell interaction suppresses sprouting via signaling to MLC2 phosphorylation. *Curr Biol*. 2009;19:668–674.
8. Legate KR, Wickstrom SA, Fassler R. Genetic and cell biological analysis of integrin outside-in signaling. *Genes Dev*. 2009;23:397–418.
9. Herbert JM, Stekel D, Sanderson S, Heath VL, Bicknell R. A novel method of differential gene expression analysis using multiple cDNA libraries applied to the identification of tumour endothelial genes. *BMC Genomics*. 2008;9:153.
10. Chiang SH, Hou JC, Hwang J, Pessin JE, Saltiel AR. Cloning and functional characterization of related TC10 isoforms, a subfamily of Rho proteins involved in insulin-stimulated glucose transport. *J Biol Chem*. 2002;277:13067–13073.
11. Vignal E, De Toledo M, Comunale F, Ladopoulou A, Gauthier-Rouviere C, Blangy A, Fort P. Characterization of TCL, a new GTPase of the rho family related to TC10 andCcdc42. *J Biol Chem*. 2000;275:36457–36464.
12. Chang L, Chiang SH, Saltiel AR. Insulin signaling and the regulation of glucose transport. *Mol Med*. 2004;10:65–71.
13. Abe T, Kato M, Miki H, Takenawa T, Endo T. Small GTPase Tc10 and its homologue RhoT induce N-WASP-mediated long process formation and neurite outgrowth. *J Cell Sci*. 2003;116:155–168.
14. Aspenstrom P, Fransson A, Saras J. Rho GTPases have diverse effects on the organization of the actin filament system. *Biochem J*. 2004;377:327–337.
15. Nishizuka M, Arimoto E, Tsuchiya T, Nishihara T, Imagawa M. Crucial role of TCL/TC10beta L, a subfamily of Rho GTPase, in adipocyte differentiation. *J Biol Chem*. 2003;278:15279–15284.
16. de Toledo M, Senic-Matuglia F, Salamero J, Uze G, Comunale F, Fort P, Blangy A. The GTP/GDP cycling of rho GTPase TCL is an essential regulator of the early endocytic pathway. *Mol Biol Cell*. 2003;14:4846–4856.
17. Vernon RB, Sage EH. Contraction of fibrillar type I collagen by endothelial cells: a study in vitro. *J Cell Biochem*. 1996;60:185–197.
18. Piette D, Hendrickx M, Willems E, Kemp CR, Leyns L. An optimized procedure for whole-mount in situ hybridization on mouse embryos and embryoid bodies. *Nat Protoc*. 2008;3:1194–1201.
19. Holthofer H, Virtanen I, Kariniemi AL, Hormia M, Linder E, Miettinen A. Ulex europaeus I lectin as a marker for vascular endothelium in human tissues. *Lab Invest*. 1982;47:60–66.
20. Walls JR, Coultas L, Rossant J, Henkelman RM. Three-dimensional analysis of vascular development in the mouse embryo. *PLoS One*. 2008;3:e2853.
21. Sadler JE. Biochemistry and genetics of von Willebrand factor. *Annu Rev Biochem*. 1998;67:395–424.
22. Clemens MJ. Translational control in virus-infected cells: models for cellular stress responses. *Semin Cell Dev Biol*. 2005;16:13–20.
23. Espert L, Rey C, Gonzalez L, Degols G, Chelbi-Alix MK, Mechti N, Gongora C. The exonuclease ISG20 is directly induced by synthetic dsRNA via NF-kappaB and IRF1 activation. *Oncogene*. 2004;23:4636–4640.
24. Bishop ET, Bell GT, Bloor S, Broom IJ, Hendry NF, Wheatley DN. An in vitro model of angiogenesis: basic features. *Angiogenesis*. 1999;3:335–344.
25. Donovan D, Brown NJ, Bishop ET, Lewis CE. Comparison of three in vitro human 'angiogenesis' assays with capillaries formed in vivo. *Angiogenesis*. 2001;4:113–121.
26. Ferrara N. VEGF and the quest for tumour angiogenesis factors. *Nat Rev Cancer*. 2002;2:795–803.
27. Garrett TA, Van Buul JD, Burridge K. VEGF-induced Rac1 activation in endothelial cells is regulated by the guanine nucleotide exchange factor Vav2. *Exp Cell Res*. 2007;313:3285–3297.
28. Adams RH, Eichmann A. Axon guidance molecules in vascular patterning. *Cold Spring Harb Perspect Biol*. 2010;2:a001875.
29. Straight AF, Cheung A, Limouze J, Chen I, Westwood NJ, Sellers JR, Mitchison TJ. Dissecting temporal and spatial control of cytokinesis with a myosin II Inhibitor. *Science*. 2003;299:1743–1747.
30. Jain RK. Normalization of tumor vasculature: an emerging concept in antiangiogenic therapy. *Science*. 2005;307:58–62.
31. Vicente-Manzanares M, Ma X, Adelstein RS, Horwitz AR. Non-muscle myosin II takes centre stage in cell adhesion and migration. *Nat Rev Mol Cell Biol*. 2009;10:778–790.
32. Parsons JT, Horwitz AR, Schwartz MA. Cell adhesion: integrating cytoskeletal dynamics and cellular tension. *Nat Rev Mol Cell Biol*. 2010;11:633–643.

Supplement Material

RhoJ/TCL regulates endothelial motility and tube formation and modulates actomyosin contractility and focal adhesion numbers

Sukhbir Kaur, Katarzyna Leszczynska, Sabu Abraham, Margherita Scarcia, Sabina Hiltbrunner, Christopher J Marshall, Georgia Mavria, Roy Bicknell and Victoria L. Heath
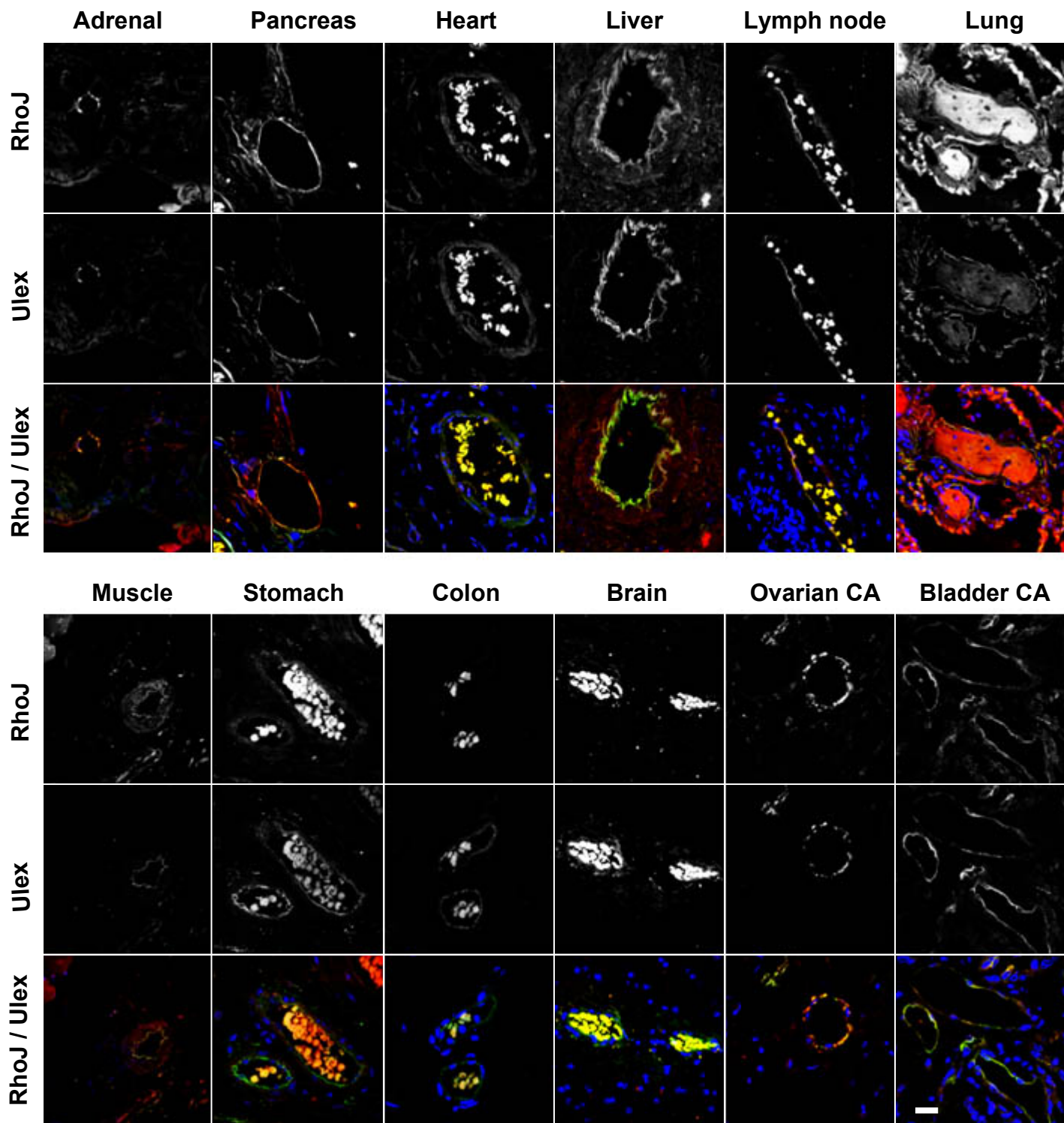
Figure I: Tissue distribution of RhoJ expression
Fluorescence *in situ* hybridisation was performed on a variety of normal and cancerous human tissue sections using digoxigenin labelled RhoJ specific riborprobe (red) and *Ulex europeaus* agglutinin I to stain the endothelial cells (green). Nuclei were stained using DAPI (blue). Erythrocytes which are found in vessels in some tissue sections autofluoresce in both the red and green channels. Scale bar represents 20 µm.

A
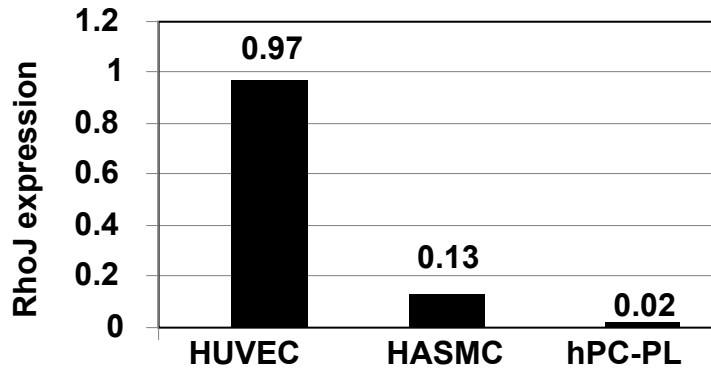
B
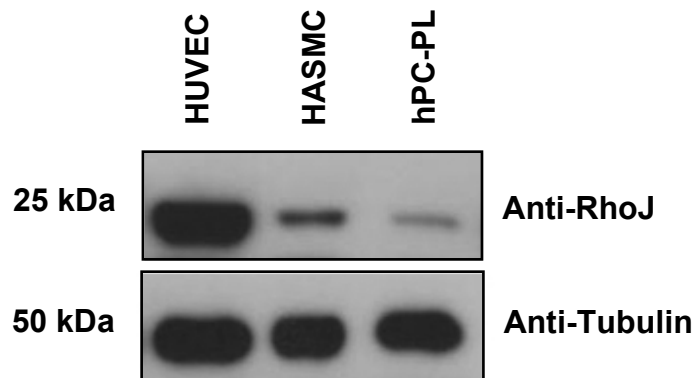
Figure II: RhoJ is expressed at low levels in pericytes and aortic smooth muscle cells
A RNA was isolated from human umbilical vein endothelial cells (HUVEC), human aortic smooth muscle cells (HASMC) and pericytes isolated from human placenta (hPC-PL). Reverse transcription and probe-based quantitative PCR was undertaken to determine levels of RhoJ and β-actin expression. The graph shows expression of RhoJ normalised to β-actin expression. The numbers show the values. **B** Cellular extract from HUVEC, HASMC and hPC-PL were subjected to SDS-PAGE and western blotting with anti-RhoJ and anti-tubulin antibodies. This experiment was performed on single isolates of each cell type.
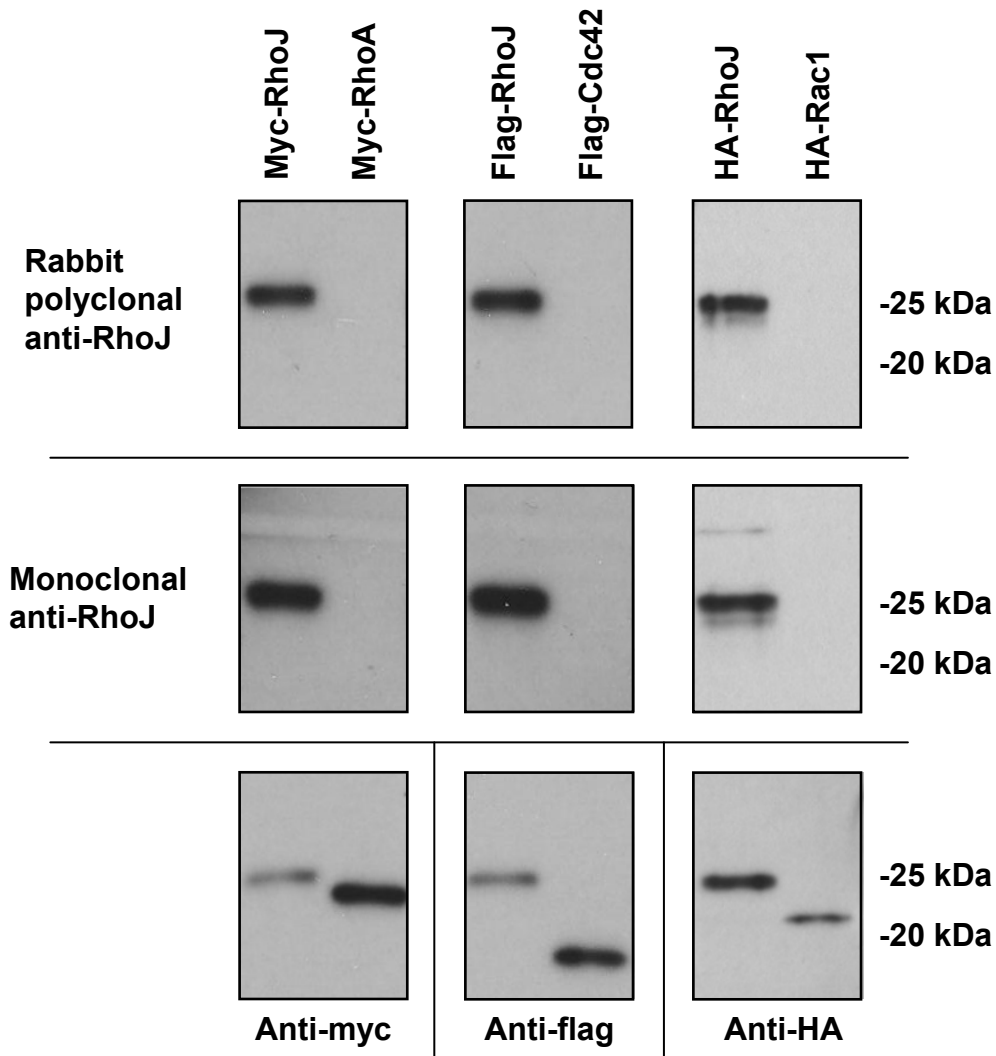
Figure III: The anti-RhoJ monoclonal and rabbit polyclonal antibodies do not detect Cdc42, RhoA or Rac1 by western blotting

Embryonic kidney HEK293 cells, which do not express RhoJ, were transfected with plasmids in order to express myc-(da)RhoA, flag-Cdc42, HA-Rac1, as well as RhoJ tagged with the same epitopes. Lysates were prepared, subjected to SDS-PAGE and western blotted with different antibodies as indicated. The epitope tagged RhoA, Cdc42 and Rac1 were not detected by either the monoclonal or rabbit polyclonal anti-RhoJ antibodies. This experiment was performed once.
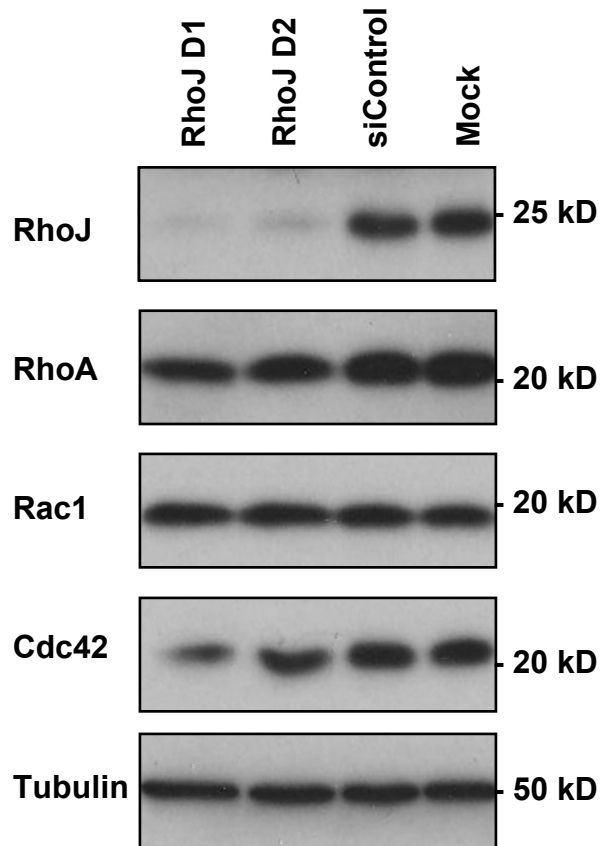
Figure IV: Knockdown of RhoJ expression does not alter expression of RhoA, Cdc42 or Rac1

HUVEC were either mock transfected or transfected with siControl or RhoJ siRNA duplexes D1 or D2 at 25 nM. Two days after transfection, cells were harvested, lysed and subjected to SDS-PAGE and western blotting for RhoJ, RhoA, Cdc42, Rac1 or tubulin. This is representative of data from three experiments.

A

B
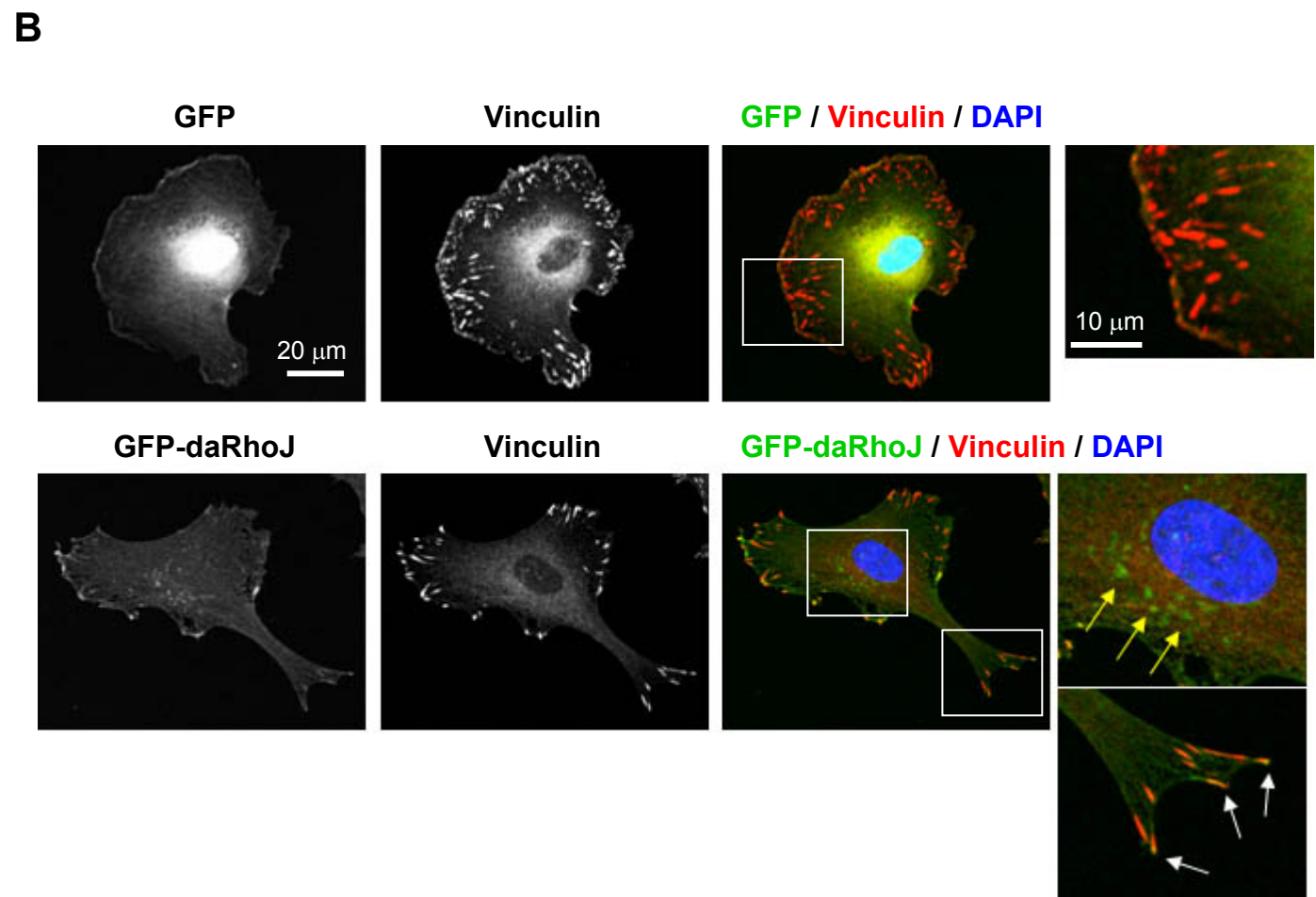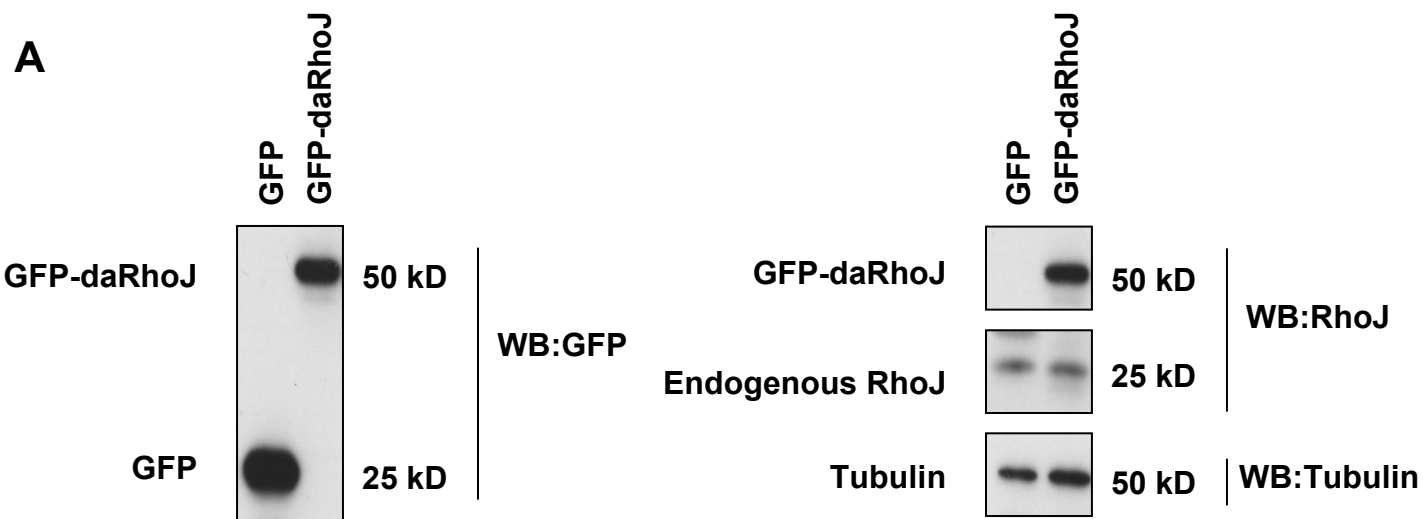
Figure V: Expression and localisation of GFP-daRhoJ
HUVEC were transduced with lentivirus to express either GFP or GFP-daRhoJ, GFP positive cells were purified by flow cytometric sorting. **A** Western blots of lysates from HUVEC expressing either GFP or GFP-daRhoJ, blotted for GFP, RhoJ or tubulin. **B** Cells were plated and immunofluorescence with anti-vinculin antibody was performed to visualise the focal adhesions. The nuclei were stained with DAPI. The region in the white box is expanded to give a more detailed view of these areas of the cell. GFP-daRhoJ localised to the membrane where it is concentrated in focal adhesions (white arrows) as well as being found in intracellular vesicles (yellow arrows). These data are representative of three experiments.
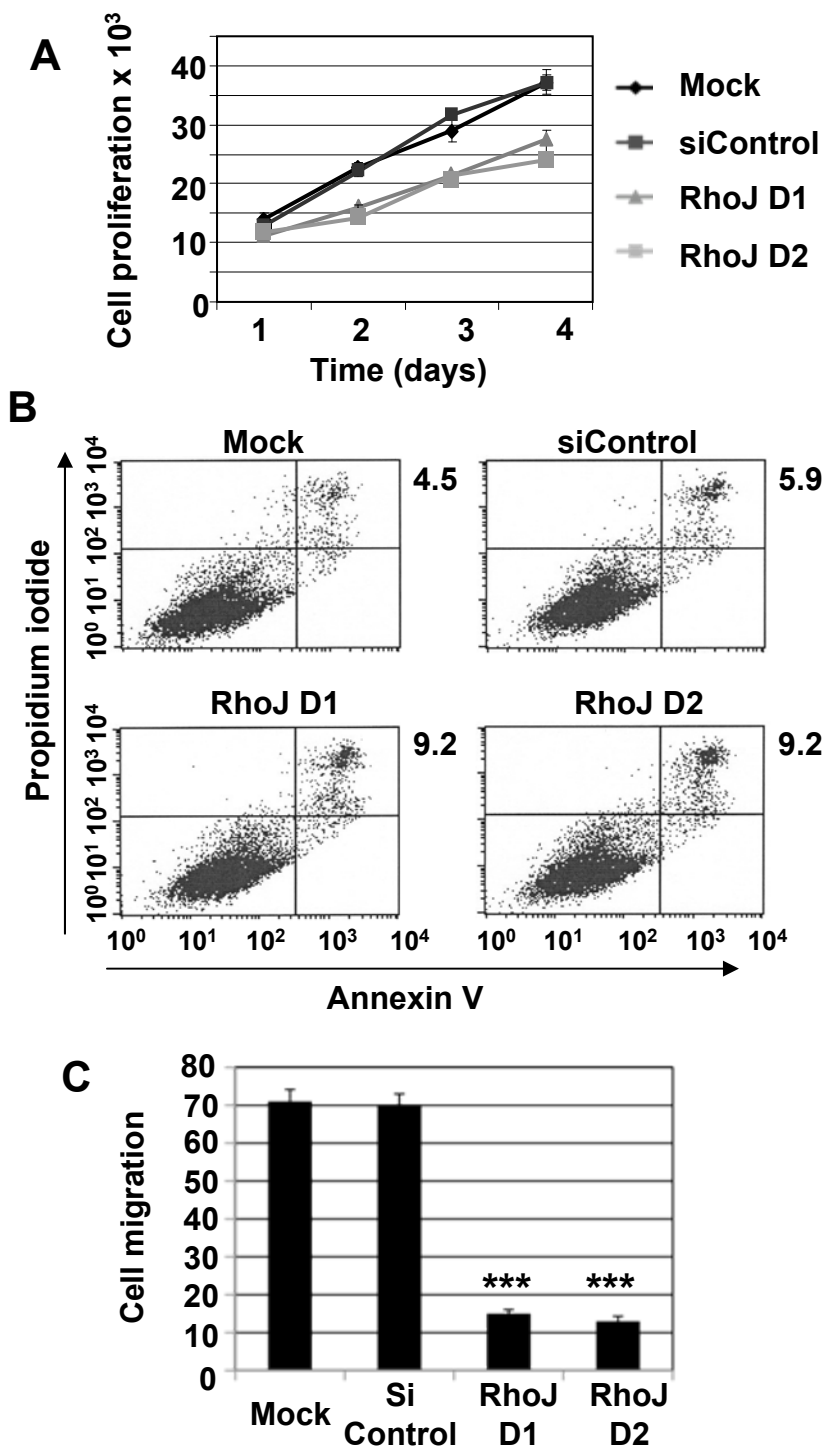
Figure VI: RhoJ regulates endothelial cell growth, survival and chemotaxis
HUVEC were either mock transfected or transfected with siControl, RhoJ D1 or RhoJ D2 siRNA duplexes at 10 nM. **A** Cell growth was assessed by cell counting each day after transfection. Error bars represent the standard error of the triplicates for each time point. **B** Three days after transfection, cells were stained with Annexin V and Propidium iodide (PI) and analysed by a Fluorescence Activated Cell Scanner. The percentage of cells stained double positive for both Annexin V and propidium iodide is indicated. These data are representative of three experiments. **C** Two days after transfection, a Boyden chamber chemotaxis assay was performed and the number of migrated cells quantified. The error bars represent the standard error of the mean, RhoJ knockdown with either RhoJ D1 or RhoJ D2 resulted in a highly significant reduction in chemotaxis (*** $p < 0.0001$ comparing RhoJ D1 or RhoJ D2 with siControl using a Mann-Whitney Test).

A

B
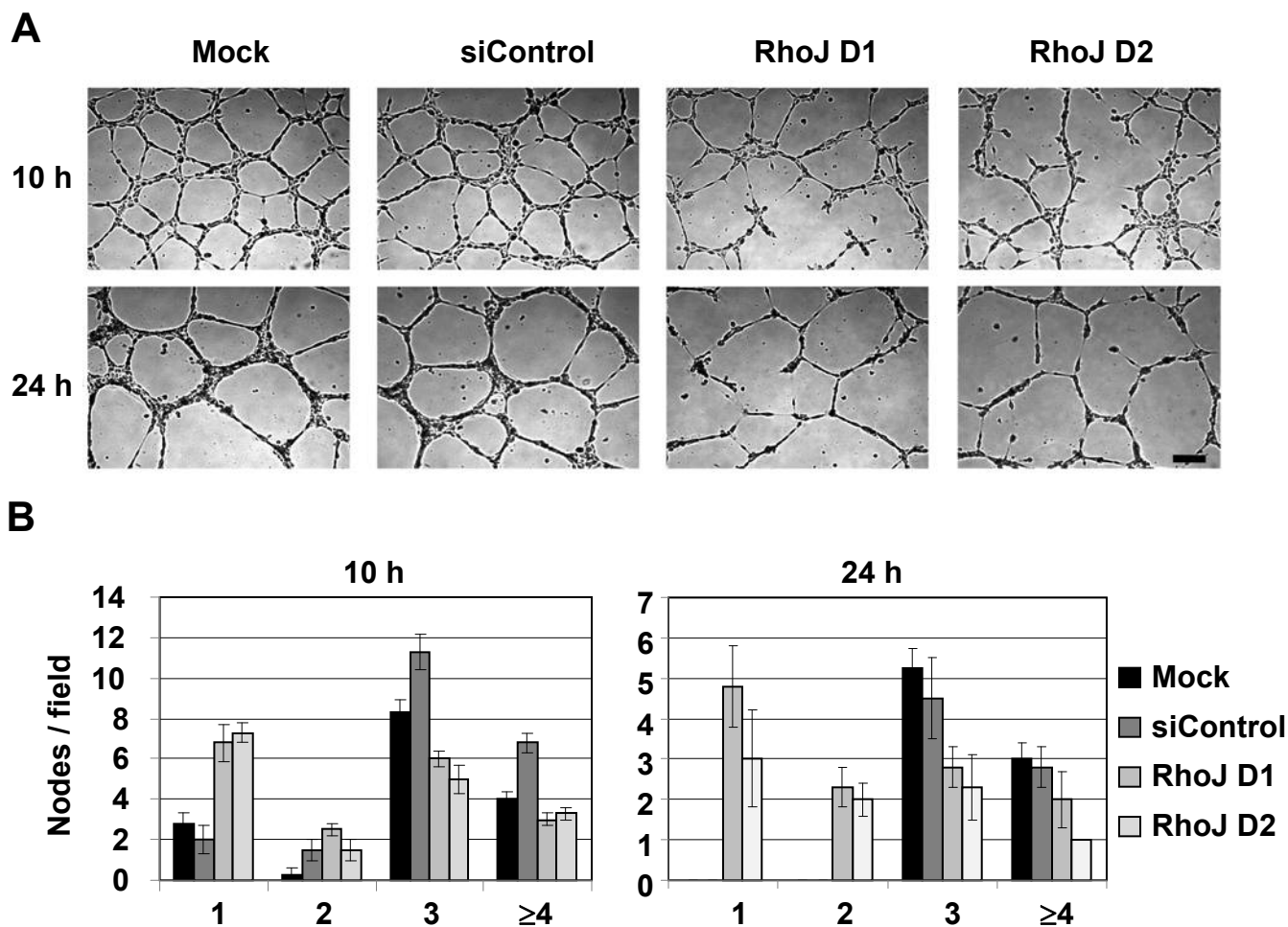
Figure VII: RhoJ mediates 2-dimensional endothelial tube formation on matrigel
A HUVEC were either mock transfected or transfected with siControl or RhoJ siRNA
duplexes D1 or D2 at 10 nM. Two days after transfection, cells were plated on to matrigel and
incubated for a further 24 hours. Pictures were taken at 10 and 24 hours. Scale bar represents
200 μm. **B** The matrigel assays were quantified by counting the number of nodes with 1, 2, 3
or 4 branchpoints from five fields of view from one representative experiment. The mean
number of nodes per field is shown and error bars represent standard error of the mean. These
data are representative of three experiments.
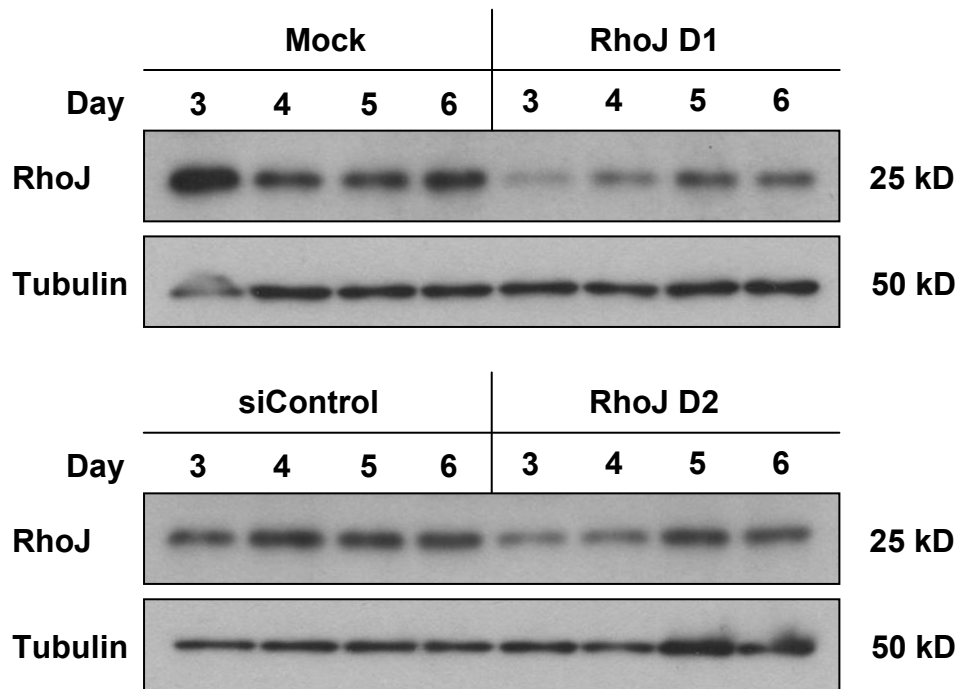
Figure VIII: Analysis of RhoJ knockdown at 3 – 6 days post transfection
HUVEC were transfected with siControl or RhoJ siRNA duplexes D1 or D2 at 20 nM using Genefector reagent. Cells were harvested at days 3, 4, 5 and 6 after transfection, lysates prepared and protein concentrations determined. 10 µg of protein extract per sample was subjected to SDS-PAGE and western blotting with anti-RhoJ and anti-tubulin antibodies. Densitometry of this blot demonstrates that for RhoJ D1 and D2 there was approximately 60% and 40% knockdown of RhoJ, respectively, persisting at 4 days after transfection.
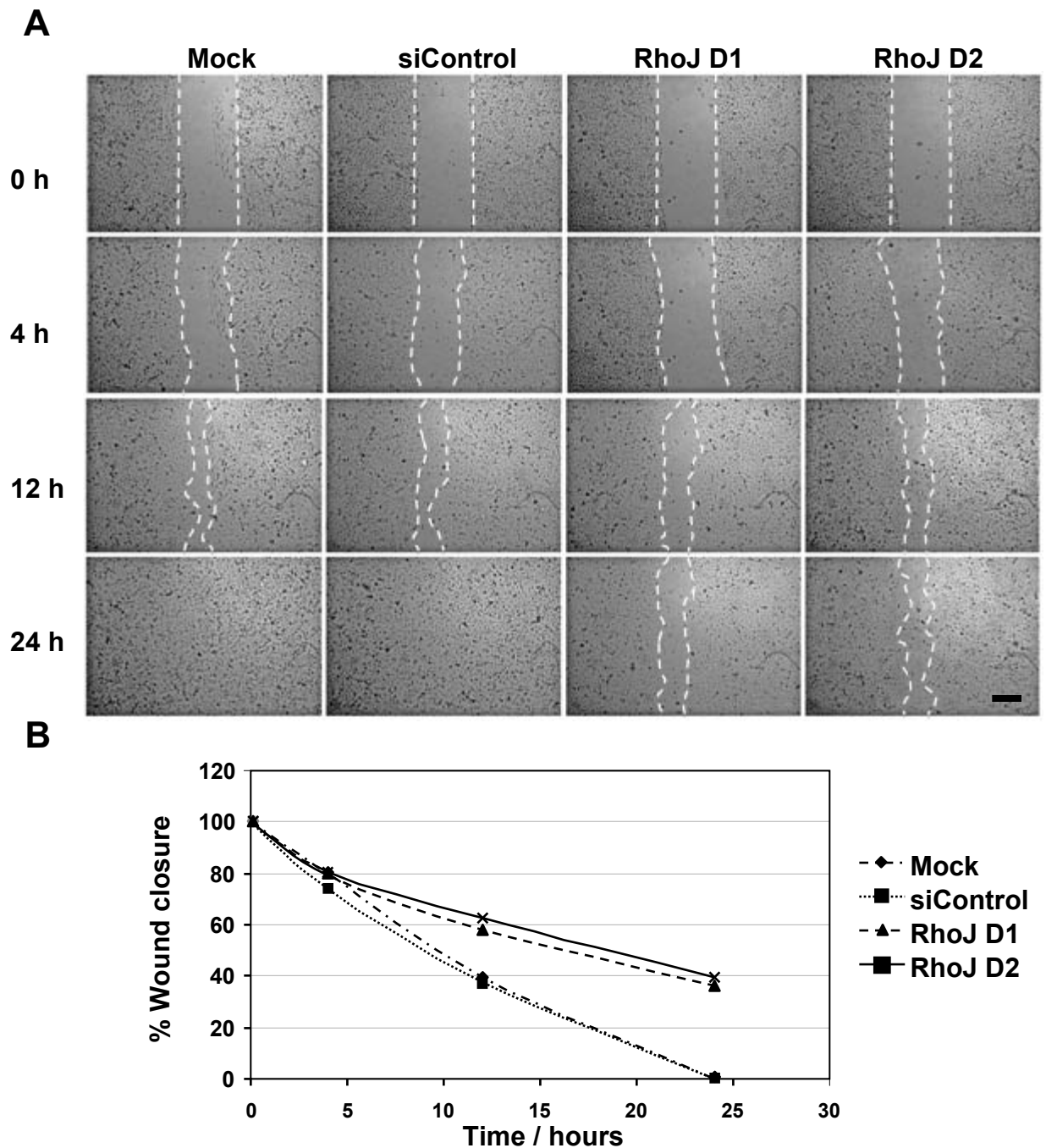
Figure IX: Knockdown of RhoJ reduces endothelial motility in the microvascular cell line HMEC-1
A HMEC-1 cells were either mock transfected or transfected with negative control duplex (siControl), RhoJ duplex 1 (D1) or RhoJ duplex 2 (D2) at 10 nM. A scratch was made two days after transfection and the scratch was imaged at time 0, 4, 12 and 24 hours. Scale bar represents 200 μm. **B** Quantitation of the wound closure. This experiment was performed once with this endothelial cell line.
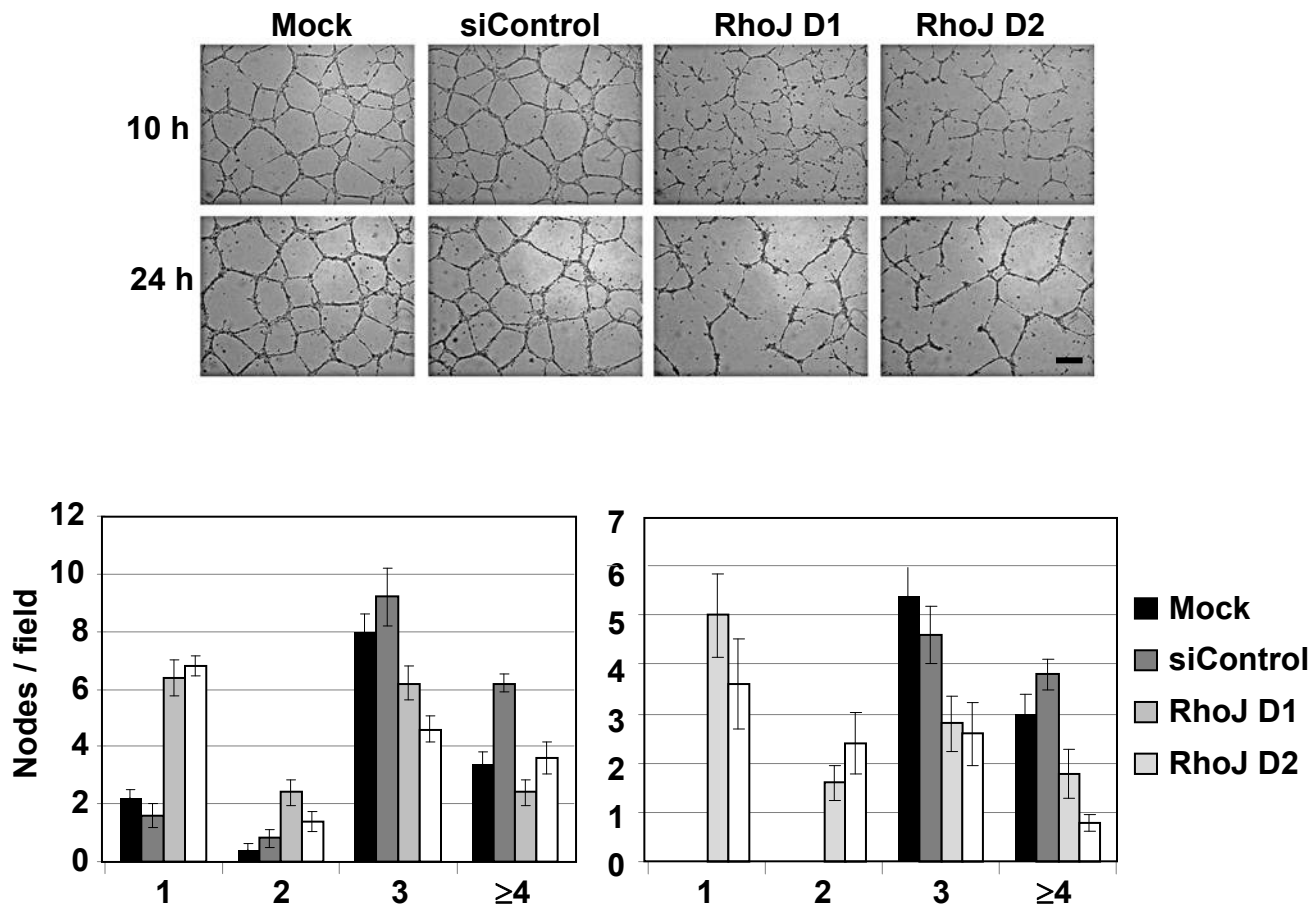
Figure X: RhoJ regulates 2-dimensional tube formation in a microvascular cell line HMEC-1

A HMEC-1 were either mock transfected or transfected with the siControl or RhoJ siRNA duplexes D1 or D2 at 10 nM. Two days after transfection, cells were plated on to matrigel and incubated for a further 24 hours. Pictures were taken at 10 and 24 hours. Scale bar represents 200 μm. **B** The matrigel assays were quantified by counting the number of nodes with 1, 2, 3 or 4 branchpoints from five fields of view from one representative experiment. The mean number of nodes per field is shown and error bars represent standard error of the mean. This experiment was performed once with this endothelial cell line.
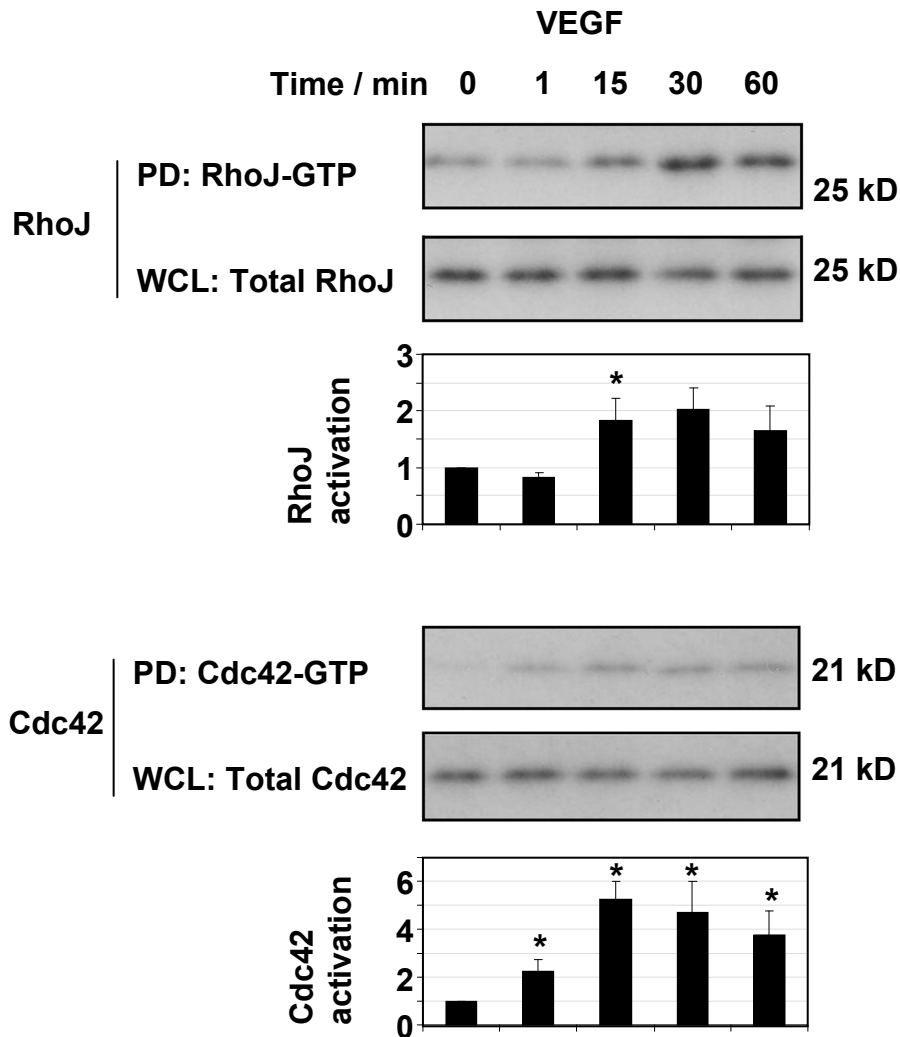
Figure XI: RhoJ and Cdc42 are activated by VEGF-A in HUVEC
HUVEC were stimulated with VEGF-A (10 ng/ml) for the times indicated. Active RhoJ
(GTP-RhoJ) or Cdc42 (GTP-Cdc42) were determined by pull-down (PD) with GST-PBD and
western blotting. The whole cell lysates (WCL) were blotted as a loading control.
Densitometry was performed on these western blots and amount of activated RhoGTPase
plotted relative to total RhoGTPase, with the zero time point normalized to 1. The graphs
show the mean and standard error of the mean derived from 5 experiments using different
donors. Using the Wilcoxon signed-rank test all time points for Cdc42 and the 15 minute
time point for RhoJ were statistically significant ($p < 0.05$), these are indicated by an *.
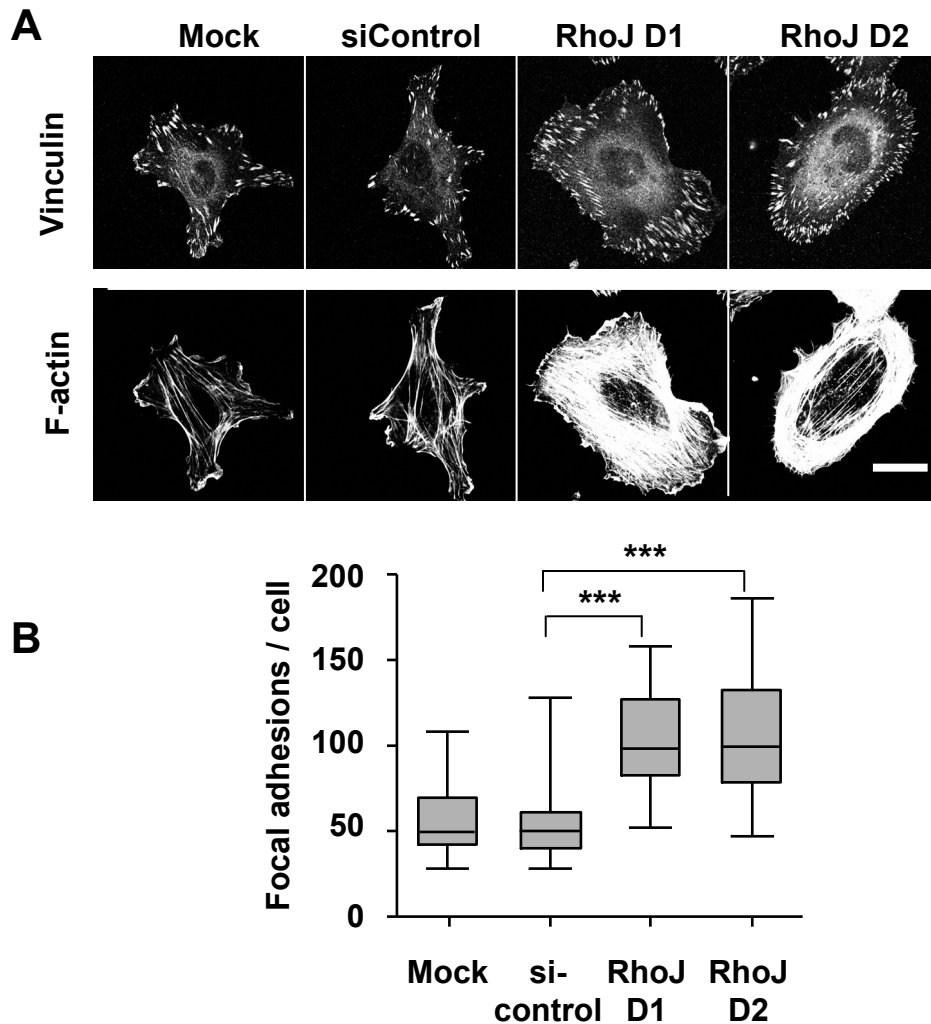
Figure XII: Knocking down RhoJ expression increases stress fibres, focal adhesions and actomyosin contractility

A HUVEC were transfected with RhoJ D1, RhoJ D2, siControl siRNA at 10 nM or mock transfected. Two days after transfection, cells were plated at low density on to gelatin coated coverslips and stained to visualise f-actin (phalloidin) and focal adhesions (anti-vinculin). This data is representative of three experiments. Scale bar represents 20 μm. **B** The number of focal adhesions per cell was quantified for 30 cells from 3 experiments and displayed as a box and whisker plot, this indicates the maximum, minimum, 25th and 75th percentiles and median values. Focal adhesion number was significantly increased by RhoJ knockdown (p < 0.001 comparing D1 or D2 with siControl using a Mann Whitney test).
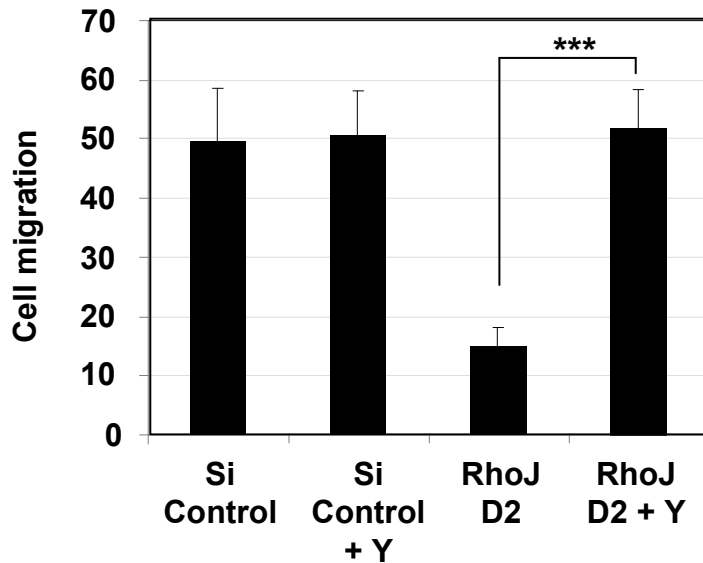
Figure XIII: Inhibition of ROCK restores chemotaxis in RhoJ siRNA treated HUVEC

HUVEC were transfected with either 10n M siScramble or RhoJ D2. A Boyden chamber chemotaxis assay was set up two days later at which point groups were divided and treated either with (+Y) or without ROCK kinase inhibitor Y27632. The number of migrated cells were quantified. The error bars represent the standard error of the mean, *** $p = 0.0006$ comparing RhoJ D2 with RhoJ D2 + Y27632 using a Mann Whitney test. Scale bar represents 200 μm.
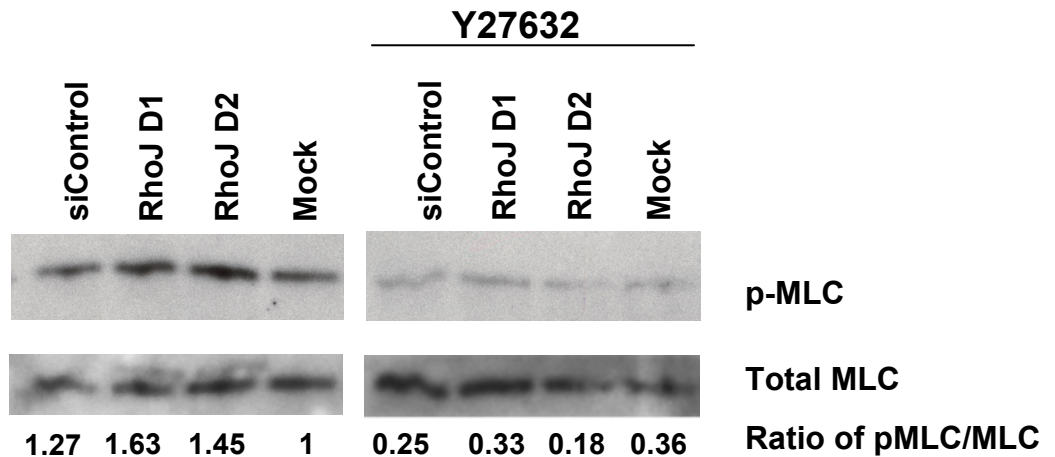
Figure XIV: Inhibition of ROCK reduces phospho-MLC in both control HUVEC and HUVEC with reduced RhoJ expression

HUVEC were transfected with RhoJ D1, RhoJ D2, siControl at 10 nM or mock transfected. One day after transfection, cells were replated on matrigel either with or without the ROCK kinase inhibitor Y27632 at 10 µM, after 24 hours cell lysate was prepared and blotted for phospho and total MLC. This experiment was performed once.
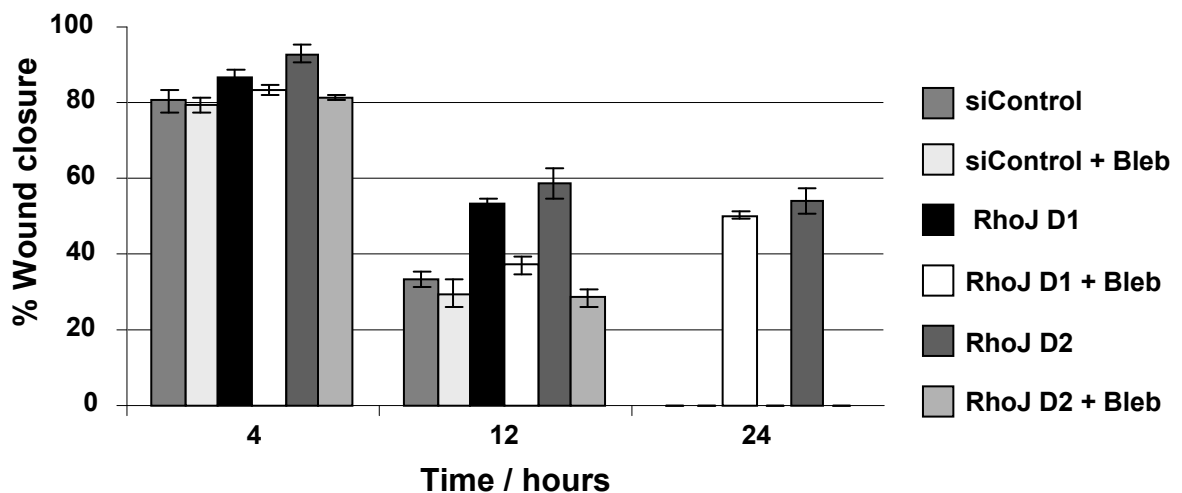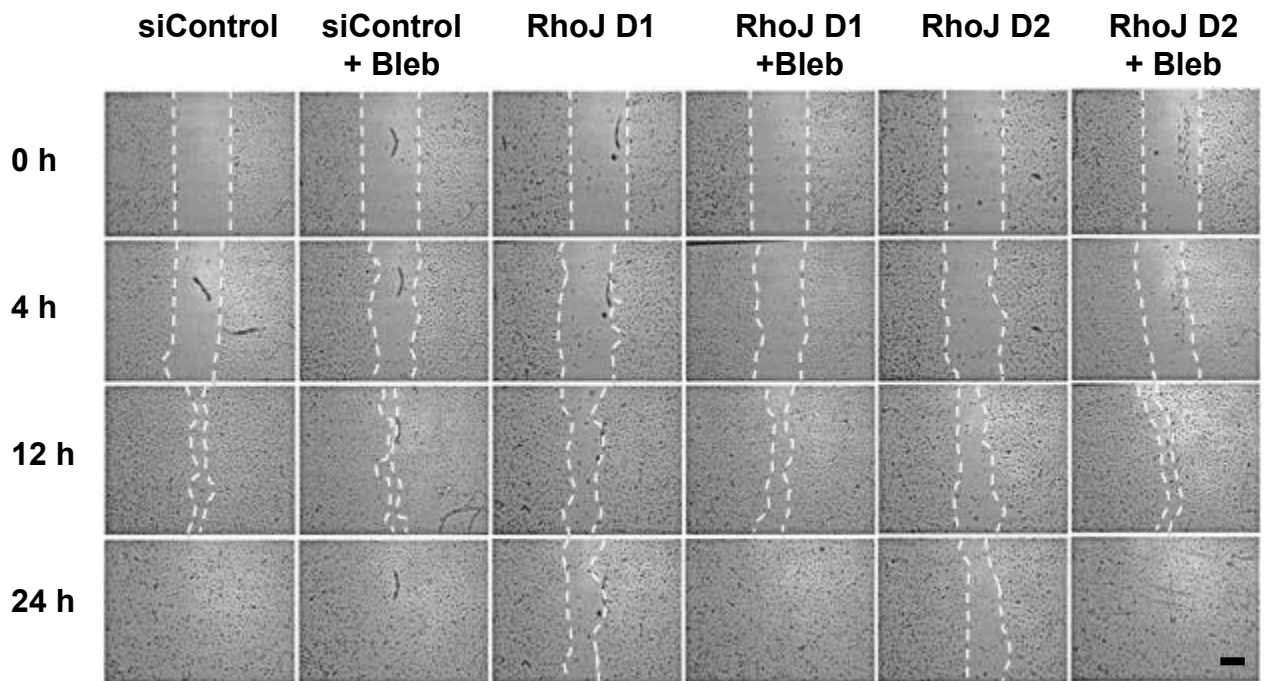
Figure XV: Inhibition of non-muscle myosin restores migration in RhoJ siRNA treated HUVEC

HUVEC were transfected with either siControl, RhoJ D1 or RhoJ D2 at 10 nM. Assays were set up two days later at which point groups were divided and treated either with (+Bleb) or without the non-muscle myosin inhibitor blebbistatin at 5 µM. These data are representative of three experiments. **A** The Scratch wound assay was performed and the cells were visualised at 0, 4, 12 and 24 hours. Scale bar represents 200 µm. **B** The percentage wound closure was measured for three independent experiments and plotted, error bars represent the standard error of the mean.
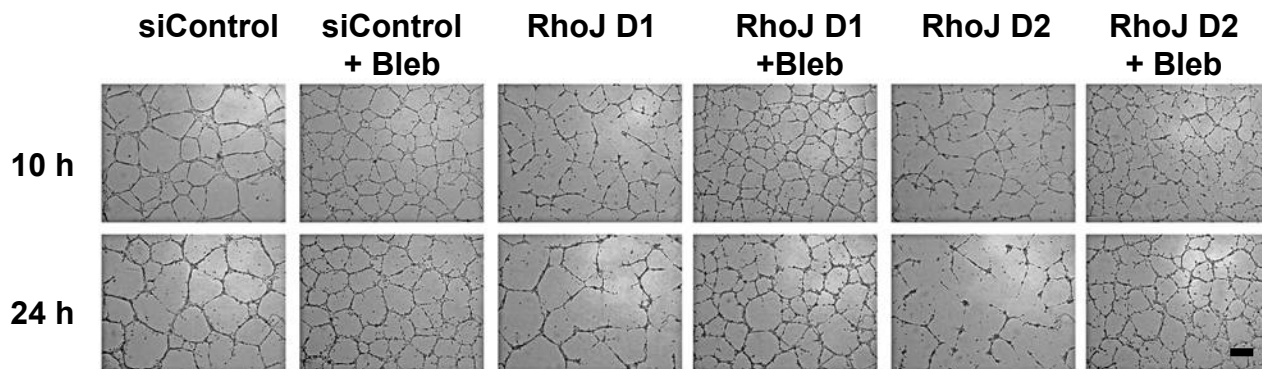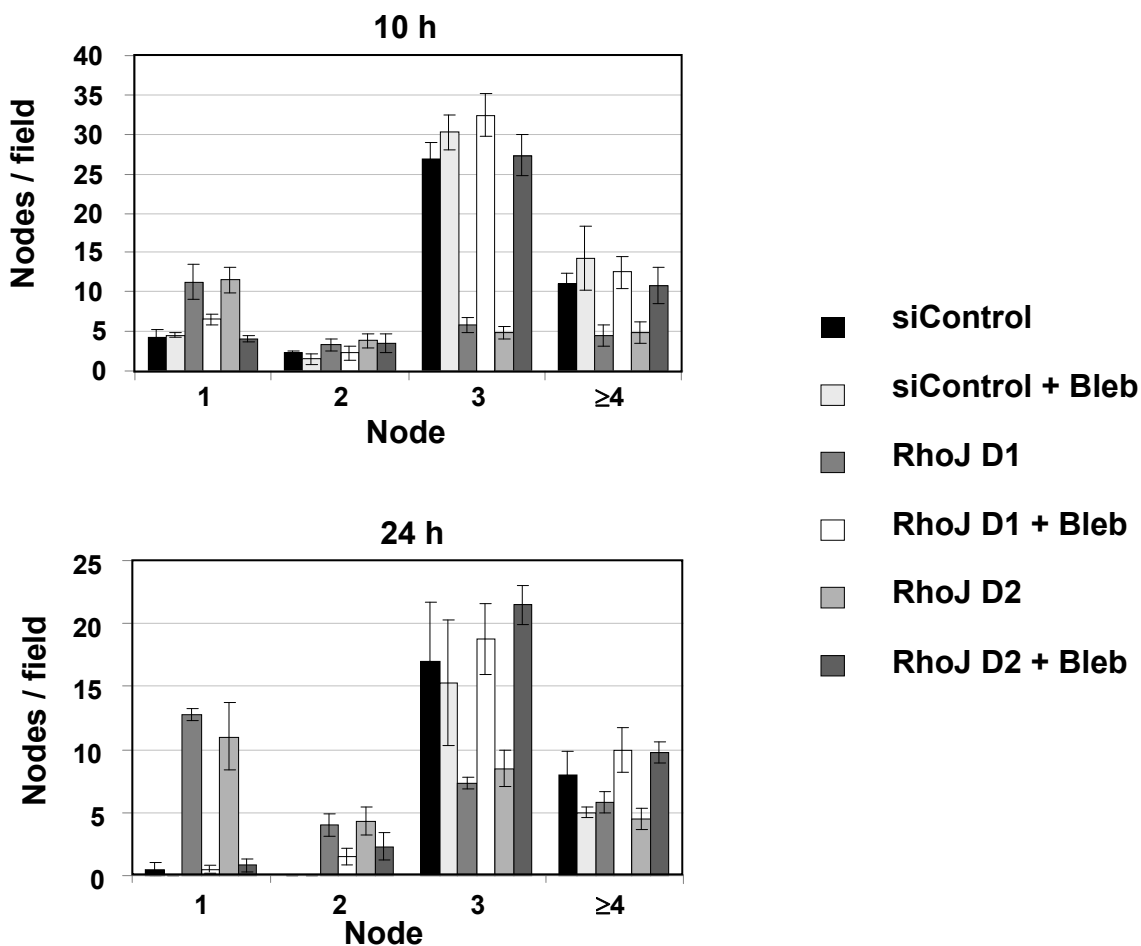
Figure XVI: Inhibition of non-muscle myosin restores tube formation in RhoJ siRNA treated HUVEC

HUVEC were transfected with either siControl, RhoJ D1 or RhoJ D2 at 10 nM. Assays were set up two days later at which point groups were divided and treated either with (+Bleb) or without the non-muscle myosin inhibitor blebbistatin at 5 μM. **A** Cells were plated on to matrigel and images taken 10 and 24 hours later. Scale bar represents 200 μm. **B** The matrigel assays were quantified by counting the the number of nodes with 1, 2, 3 or 4 branchpoints from five fields of view from one representative experiment. The mean number of nodes per field is shown and error bars represent standard error of the mean.

Full legends

Figure 1: RhoJ has a vascular expression pattern

A Fluorescent *in situ* hybridization on a human tissue sections using digoxigenin labelled riboprobes/anti-digoxigenin-rhodamine (red) in combination with *Ulex europeaus* agglutinin I-fluorescein (green). **B** Whole-mount *in situ* hybridization experiments were performed on E9.5 mouse embryos using full length mouse RhoJ antisense and sense riboprobes. Von Willebrand Factor (VWF) riboprobes were also used as a positive control for endothelial cell expression. There is a magnified image of both the sense and antisense hybridization; white arrows indicate the intersomitic vessels and the yellow arrows mark the dorsal aorta. This is representative of three experiments. **C** Immunofluorescence staining of HUVEC using anti-mouse RhoJ (green) and anti-vinculin or anti-phospho-FAK (Y397) (red). Nuclei were counterstained with DAPI. There is a magnified image showing co-localisation. This was repeated with at least three different isolates of HUVEC.

Figure 2: RhoJ regulates endothelial cell motility

A, C, E HUVEC were either mock transfected or transfected with siControl or RhoJ siRNA duplexes D1 or D2 at 10 nM. **A** Two days after transfection, scratches were made and the cells visualised at 0, 4, 12 and 24 h. **C** The percentage of the wound remaining at different time points was measured from three independent experiments and the mean plotted with error bars denoting the standard error. Statistically significant differences were observed at the 24 hour time point by comparing RhoJ D1 and D2 transfected cells with the siScramble control transfected cells by the Student T test (** $p= 0.001$ to 0.01 and * $p=0.01$ to 0.05.) **E** Western blot of transfected HUVEC was performed using anti-RhoJ and anti-tubulin antibodies to demonstrate RhoJ

knockdown. **B, D, F** HUVEC were transduced with lentivirus and and sorted to generate populations of HUVEC expressing either GFP (control) or GFP-daRhoJ. Scratch wound assays were performed and the cells visualised at 0, 4, 8 and 12 h. **D** The percentage of the wound remaining at different time points was measured from three independent experiments and the mean plotted with error bars denoting the standard error. **F** A western blot using anti-GFP antibodies to show expression of GFP and GFP-daRhoJ. These data are representative of three experiments.

Figure 3: RhoJ mediates endothelial tube formation

A, B RhoJ knockdown inhibits tubule formation. HUVEC were either mock transfected or transfected with siControl or RhoJ siRNA duplexes D1 or D2 at 20 nM. A day after transfection they were seeded on to confluent HDF and cultured for a further 5 days to allow tubules to develop, these were visualised by staining with anti-CD31. **B** Tubule length, number and the number of junctions were quantified using the AngioSys software from at least 9 fields of view, all were highly significantly reduced as a result of RhoJ knockdown ($p < 0.001$ comparing RhoJ D1 or RhoJ D2 with siControl using a Mann Whitney test). **C, D** Expression of GFP-daRhoJ promotes tubule sprouting. HUVEC were transduced with lentivirus to express GFP or GFP-daRhoJ and GFP positive cells were purified by cell sorting. These were then plated on HDF as described above. **D** Total tubule length, mean tubule length, tubule number and the number of junctions per field were quantified using the Angiosys software. Data plotted represent the mean of 9 fields and error bars represent the standard error. Expression of daRhoJ increased the number of junctions and tubules compared with the GFP control, but resulted in a reduction in the mean tubule length (using a Mann Whitney test comparing control GFP were compared with

GFP-daRhoJ, *** p<0.001, ** p= 0.001 to 0.01 and * p=0.01 to 0.05.) These data are representative of three experiments.

Figure 4: RhoJ activity regulates focal adhesion number

A HUVEC were transfected with RhoJ D1, RhoJ D2, siControl siRNA at 10 nM duplex or mock transfected or lentivirally transduced to express GFP or GFP-daRhoJ.   Scratch wound assays were set up, cells were allowed to migrate, and were then fixed and focal adhesions visualised using anti-vinculin immunofluorescence. These data are representative of three experiments.

B Focal adhesion numbers in cells at the scratch margin were quantified for at least 20 cells from 3 experiments and displayed as a box and whisker plot, this indicates the maximum, minimum, 25th and 75th percentiles and median values. Focal adhesion number was significantly increased by RhoJ knockdown and significantly decreased by expression of GFP-daRhoJ (p < 0.001 comparing RhoJ D1 or RhoJ D2 with siControl and also by comparing GFP with GFP-daRhoJ using a Mann Whitney test).

Figure 5: RhoJ influences stress fibres and actomyosin contractility. HUVEC were transfected with RhoJ D1, RhoJ D2, siControl siRNA duplex at 10 nM or mock transfected (A, B, E, F) or lentivirally transduced to express GFP or GFP-daRhoJ (C, D, E).   **A, C** Scratch wound assays were set up and the cells allowed to migrate, cells were then fixed and f-actin visualised by staining with phalloidin-TRITC. These data are representative of three experiments. **B, D** The fluorescence intensity/cell in cells at the wound edge was quantified from at least 20 cells from 3 experiments and displayed as a box and whisker plot, this indicates the maximum, minimum, 25th and 75th percentiles and median values. The fluorescence/cell was

significantly increased by RhoJ knockdown and significantly decreased by expression of GFP-daRhoJ (p < 0.001 comparing RhoJ D1 or RhoJ D2 with siControl and also by comparing GFP with GFP-daRhoJ using a Mann Whitney test). **E** Collagen gel contraction assays were set up using siRNA duplex transfected HUVEC or lentivirally transduced HUVEC as noted above, for both the siRNA and lentiviral transduction, three different donor HUVEC were used. For each condition a control was added where the non-muscle myosin II was inhibited by blebbistatin at 5 µM. The mean of data from each donor is plotted and error bars represent the standard error, pairs of data were compared with a Student T test as indicated *** p<0.001, ** p= 0.001 to 0.01 and * p=0.01 to 0.05. **F** One day after transfection with siRNA duplexes, cells were replated on matrigel, after 24 hours cell lysates were prepared and blotted for phospho- and total MLC. Increased phopho-MLC (p-MLC) in RhoJ siRNA treated cells was observed in three experiments.

Figure 6: Inhibition of ROCK restores migration and tube formation in RhoJ siRNA treated HUVEC

HUVEC were transfected with either siControl or RhoJ D2 at 10 nM. Assays were set up two days later at which point groups were divided and treated either with or without 10 µM Y27632, a ROCK kinase inhibitor. **A** Scratch wound assays were performed and the cells were visualised at 0, 4, 12 and 24 hours. **B** The percentage of the wound remaining at different time points was measured from three independent experiments and the mean plotted with error bars denoting the standard error. Using the student T test, statistically significant differences were observed at the 12 hour time between the untreated siScramble and untreated RhoJ D2 transfected cells as well as between the RhoJ D2 transfected HUVEC treated with and without

Y27632. At 24 hours, significant differences were observed between the untreated RhoJ D2 transfected HUVEC and all the other groups (** p= 0.001 to 0.01 and * p=0.01 to 0.05). **C** Cells were plated on to matrigel and images taken 10 and 24 hours later. **D** Tube formation at 10 hours and 24 hours after plating was quantified by counting the number of nodes with 1, 2, 3 or ≥4 branch-points from five fields of view from each condition at 10 and 24 hour time points. Error bars represent standard error of the mean. These data are representative of three experiments.

Detailed methods

1   Cell lines and culture

2   Antibodies and pharmacological inhibitors

3   Plasmids

4   siRNA transfection

5   Lentiviral transduction of HUVEC

6   Expression of RhoGTPases in HEK293T cells

7   Inhibition of ROCK and non-muscle myosin II

8   Matrigel tube formation

9   Scratch wound assay

10   Cell proliferation

11   Apoptosis

12   Organotypic tube forming assay

13   Cell contraction assay

14   Immunofluorescence

1   Cell lines and culture

Human umbilical vein endothelial cells (HUVEC) were used between passage 1 and 6 for all experiments. Umbilical cords were obtained from either TCS CellWorks or Birmingham Women's Health Care NHS Trust after delivery; mothers had given informed consent. HUVEC were cultured to confluence in Media 199 (Sigma) containing 4 mM L-glutamine (Sigma), 90 µg/ml heparin (Sigma), 10% (v/v) fetal bovine serum (PAA, The Cell Culture Co) supplemented with either purified bovine brain extract [1] or large vessel endothelial growth supplements (TCS CellWorks). Cells were plated in sterile culture dishes that had been coated with 0.1% (w/v) gelatin diluted in phosphate buffered saline (PBS). The plates were incubated in a humidified atmosphere with 5% CO_2 at 37°C. HUVEC were split at a ratio of 1:3 once a week and were

used between passages 1 to 6. The human microvascular endothelial cell line-1 (HMEC-1) [2] was

cultured in the same way as HUVEC. Human pericytes from human placenta (hPC-PL) were

obtained from Promocell and cultured in Pericyte Growth Medium (Promocell) on untreated

tissue culture plastic, and used between passage 2-4. Human aortic smooth muscle cell lines

(HASMC) were purchased from TCS Cell Works and cultured in Dulbecco's Modified Eagle's

Medium (DMEM) supplemented with 4 mM L-glutamine (Sigma), Pencillin Streptomycin

Solution (Sigma) and 10% (v/v) fetal bovine serum (PAA, The Cell Culture Co). These were

also cultured on untreated tissue culture plastic and used between passages 2-4. Lentivirus was

produced using human embryonic kidney (HEK) 293T cells as the packaging cell line. These

cells were cultured as for the HASMC.

2   Antibodies and pharmacological inhibitors

Primary antibodies used were as follows: anti-GFP (3E1 clone, CRUK), anti-RhoA (Santa Cruz

Biotechnology), anti-Rac1 (Millipore) anti-RhoJ (Abcam), anti-Tubulin (Sigma), anti-Cdc42

(BD Biosciences), anti-vinculin (Sigma), anti-VE cadherin (eBioscience), phospho-MLC2

(thr18/ser19, New England Biolabs) and pan MLC2 (Santa-Cruz). The production of the

purified rabbit anti-RhoJ polyclonal antisera is described in Section 23 below. Secondary

antibodies were anti-mouse immunoglobulin Alexa-fluor 488 (Invitrogen), anti-mouse

immunoglobulin Alexa-fluor 546 (Invitrogen), polyclonal goat anti-mouse immunoglobulins -

horseradish peroxidase (HRP) (Dako Cytomation), and polyclonal goat anti-rat immunoglobulin

conjugated to HRP (Sigma) and HRP-conjugated anti-rabbit immunoglobulin. Filamentous actin

was visualized using phalloidin-TRITC (Invitrogen). The ROCK inhibitor Y27632 (Tocris) was

used at a concentration of 10 µM and the non-muscle myosin II inhibitor blebbistatin (Tocris) was used at 5 µM.

3   Plasmids

pGEX KG-PBD was used to produce glutathione S-Transferase – Pak1 p21-binding domain (GST-PBD, the PBD encoded amino acids 1-254 of Rattus norvegicus PAK1 which encompasses the CRIB domain). In order to produce recombinant fusion protein for production and purification of RhoJ specific antisera, wild type RhoJ lacking the sequence encoding the CAAX box was cloned into the BamHI and HindIII restriction sites of pMAL2CE and BamHI and SmaI restriction sites of pGEX 4T2.

Riboprobes were synthesized from plasmids pGEM3Z-mRhoJ (mouse RhoJ 1-645 of coding region), pGEM3Z-mVWF (7838-8387 of coding region) and pGEM3Z-hRhoJ (human RhoJ 1-645 of coding region). Mouse RhoJ (1-645 of coding region) was cloned into pGEM-3z using 5'-EcoR1 and 3'HindIII restriction sites. Mouse von Willebrand Factor (VWF) (7838-8387 of coding region) was cloned into pGEM-3z plasmid using 5'-BamH1 and 3'-EcoR1 restriction sites. Human RhoJ (1-645 of coding region) was cloned into pGEM-3z plasmid using 5'-BamH1 and 3'-EcoR1 restriction sites.

The plasmids used for lentivirus production were pWPI (a lentiviral mammalian expression vector with an EMCV IRES-EGFP cassette; Addgene) or pWPXL-GFP-daRhoJ (see below) in combination with plasmids psPAX2 (Lentiviral packaging for mammalian expression; Addgene) and pMD2G (Envelope plasmid; Addgene). To generate lentivirus for expressing GFP-daRhoJ,

the constitutively active RhoJ mutant (Q79L) coding sequence was firstly cloned pEGFP-C1

using HindIII and EcoRI restriction sites (forward primer 5'-

tagtagaagctttgatgaactgcaaagagggaactgac-3', reverse primer 5'-

tagtagaagcttgaattctcagataattgaacagcagctgtg-3') to generate daRhoJ tagged at the N terminus with

GFP. Then the GFP-daRhoJ fragment was amplified from pEGFP-C1-daRhoJ (forward primer

5'- tagtagggatccgccaccatggtgagcaagggc-3', reverse primer 5'-

tagtagaagcttgaattctcagataattgaacagcagctgtg-3') and cloned into pWPXL (lentiviral mammalian

EGFP expression plasmid; Addgene) using BamHI and EcoRI restriction sites such that the

GFP-daRhoJ replaced the existing EGFP insert.

Expression plasmids for expressing epitope tagged RhoA, Rac1, Cdc42 and RhoJ were as

follows: pRK5-FLAG-Cdc42, pRK5-HA-Rac, pRK5-myc-V14RhoA and pEF6A-myc-RhoJ,

pEF6A-HA-RhoJ and pEF6A-FLAG-RhoJ.

4   siRNA transfection

For siRNA experiments the duplexes were as follows: RhoJ siRNA duplex 1 (D1, 5'-

CCACTGTGTTTGACCACTA-3'), RhoJ siRNA duplex 2 (D2, 5'-

AGAAACCTCTCACTTACGA-3') and a negative control duplex (siControl) with no homology

to any known human sequence (all synthesized by Eurogentec). Transfections of siRNA

duplexes were performed using either RNAiMAX lipofectamine (Invitrogen) at a final

concentration of 0.3% (v/v) or GeneFECTOR™ (Venn Nova, Inc.) at a final concentration of

0.5% (v/v), with duplexes at 10-25 nM. The RNAiMAX was used for all experiments except for

the organotypic tube forming assays and the phospho/total MLC blotting. For transfecting

HUVEC in 10 cm culture dishes, 10^6 HUVEC were seeded on to gelatin-coated dishes one day before transfection. For one 10 cm dish the transfection mix was prepared by firstly mixing the appropriate amount of duplex in a final volume of 680 µl of optiMEM (Invitrogen). In a separate tube, 12 µl of RNAiMAX lipofectamine was diluted in 108 µl of optiMEM. After mixing gently, both mixtures were incubated at room temperature for 10 minutes. Then the two mixtures were combined, gently flicked and incubated for a further 10 minutes at room temperature. Meanwhile, the cells were washed twice with phosphate-buffered saline (PBS) before adding 3.2 ml OptiMEM to the 10 cm plates. The final transfection mix was then added to the plate and tilted to ensure even distribution. Mock cells were transfected using the method above but with no siRNA included. After 4 hours of incubation at 5% CO_2 at 37 °C, the transfection mix was replaced with normal HUVEC media containing no antibiotics. To transfect cells in 6 cm dishes or 6 well plates, the transfection mixes were scaled down according to their surface area.

5   Lentiviral transduction of HUVEC

Production of lentivirus

HEK293T cells were used for lentiviral production. 2.5×10^6 cells were plated in sterile culture dishes (10 cm diameter) and the next day calcium-phosphate transfections were performed as follows. 20 µg transfer vector (pWPXL-GFP-daRhoJ or pWPI (GFP)), 15 µg packaging vector (psPAX2) and 6 µg envelope vector (pMD2G) were mixed with 450 µl distilled water and 63 µl 2 M calcium chloride ($CaCl_2$ $6H_2O$) in a 5 ml tube. Then 500 µl of 2x HBS (1.6% (w/v) NaCl, 0.074% (w/v) KCl, 0.027% (w/v) Na_2HPO_4 $2H_2O$,   0.2% (w/v) dextrose, 1.0 % (w/v)HEPES; pH 7.05) was added dropwise with shaking and the mixture was incubated for 15 min at room temperature to allow precipitation to occur. Prior to addition of this transfection mixture, the

media of the plated HEK293T cells was replaced with 10 ml fresh media. The cells were then incubated in a humidified atmosphere with 5% CO_2 at 37°C for 8 hours, the transfection mixture was then removed and replaced with 5 ml of fresh medium. After 48 hrs supernatant with virus was collected, centrifuged for 5 min at 1100 rpm, cleared through 0.45 µm-pore syringe filters and stored at -80°C until use.

Infection of HUVEC

10^6 HUVEC were seeded on gelatin-coated culture 10 cm dishes (0.1% (w/v) gelatin in PBS). The next day the medium was replaced with 7.5 ml of lentivirus supernatant supplemented with 8 µg/ml polybrene (Sigma), bovine brain extract and 90µg/ml heparin. Cells were then incubated for 24 hr, after which time the lentivirus supernatant was replaced with fresh medium and cells were left to grow for 2 days. This procedure typically resulted in infection of 90% for the GFP control cells and 40-60% for those infected with the GFP-daRhoJ virus. GFP positive cells were then purified by flow cytometric sorting (MoFlo Cytomation fluorescence activated cell sorter).

6   Expression of RhoGTPases in HEK293T cells

In order to express various epitope tagged RhoGTPases HEK293T cells were transfected with 5 µg of plasmid using the calcium phosphate transfection as described above in the section on lentiviral production.

7   Inhibition of ROCK and non-muscle myosin II

The ROCK inhibitor Y27632 was used at a concentration of 10 μM and the non-muscle myosin II inhibitor was used at 5 μM. These inhibitors were added to the media, where indicated, in the matrigel tube forming assay and Boyden chamber chemotaxis assay, it was added in the scratch wound assay at the time the scratch was made.

8   Matrigel tube formation

Natural matrigel (VWR) was thawed overnight on ice at 4 °C. The wells of a 12 well plate were wetted with PBS prior to adding 70 μl of matrigel. The basement membrane extract was allowed to solidify at 37°C for 30 minutes. Cells were harvested and seeded at a density of 1.4×10^5/well in HUVEC media. Cells were then incubated at 37°C with 5% CO_2 for a further 24 hours. Tube formation was observed by taking pictures using Leica DM IL microscope and USB 2.0 2M Xli camera (Leica Microsystems, Houston). The matrigel assays were quantified by counting the number of nodes with 1, 2, 3 or 4 branch-points from five fields of view from each condition at 10 and 24 hour time points.

9   Scratch wound assay

In a 6 well plate coated with 0.1% (w/v) gelatin in PBS, HUVEC were seeded at cell density of 1.75×10^5 and left overnight. Cells were then transfected with siRNA duplexes and two days after, pen marks were made along the bottom of the wells, then with 200 μl sterile pipette tips scratches perpendicular to the pen marks were made. Cells were washed and fresh HUVEC media containing 25 μg/ml of mitomycin C (Sigma) was added. Cells were incubated at 37°C with 5% CO_2 for a further 24 hours. Cell migration was observed by taking pictures at 0, 4, 12

and 24 hours using using Leica DM IL microscope and USB 2.0 2M Xli camera. To quantify wound closure, the areas of wounds were measured using ImageJ software. For each condition the wounds at 0 hours were considered to be 100% open, the areas at subsequent time points were divided by the area measured at the 0 hour time point and the percentage of the wound still open calculated.

10   Cell proliferation

Four hours after siRNA transfection, cell were harvested and 1.5×10^4 cells were seeded in 1 ml of HUVEC media per well of a 24 well plates coated in 0.1% (w/v) gelatin in PBS. Four plates were prepared to count the cells 1-4 days after seeding. For each plate, cells from each condition were plated in triplicate. Cells were counted using a haemocytometer and DM IL microscope (Leica).

11   Apoptosis

Three days after siRNA transfection, apoptosis was assessed using the Annexin V-FITC staining kit (BD Pharmingen) according to the manufacturer's instructions. Cells were stained in a volume of 100 μl 1 x binding buffer [10 x binding buffer: 0.1 M Hepes pH 7.4, 1.4 M NaCl, 25 mM $CaCl_2$] which contained 5 μl Annexin V-FITC and propidium iodide (Sigma) at 50 ng/ml. Cells were stained in the dark for 15 minutes before being analysed by FACS-Becton Dickson FACSCalibur (Becton and Dickson, USA) to detect apoptosis. 10,000 cells were analysed per condition. Green fluorescence was detected using FL1 channel and red fluorescence was detected using FL3 channel. Cell Quest Software (version 3.1f) displayed the results as a bivariate dot plot of Annexin V (FL1) and PI (FL3) fluorescence intensity.

12   Organotypic tube forming assay

In the organotypic assay, HUVEC were co-cultured with confluent human dermal fibroblasts (HDF) in an assay as previously described [3, 4] using the Angiokit (TCS cell works). In the case of siRNA knockdown, HUVEC were transfected with siRNA duplexes using GeneFECTOR™ (Venn Nova, Inc.) a day before seeding on to HDF which had been grown to confluence for seven days. For HUVEC expressing either GFP or GFP-daRhoJ, lentivirally tranduced and GFP positive sorted HUVEC were seeded directly on to confluent HDF. The co-cultures were incubated for 5 days and the HUVEC were visualized by staining wells using a mouse anti-human CD31 Tubule Staining Kit (TCS CellWorks) according to the manufacturer's protocol. Automated analysis was performed using the AngioSys software. The number of tubules, total tubule length and number of branch points were measured in at least 9 microscopic fields.

13   Cell contraction assay

To measure physical contractility, contraction of cell-populated type I collagen gels was assessed, such an assay has been used to measure contractility of human fibroblasts [5] and endothelial cells [6]. The cell contraction assay (Cell Biolabs, Inc., UK) was set up according to the manufacturer's instructions. 24 hours after siRNA transfection, cells were harvested and resuspended in complete HUVEC medium at 3×10^6 cells/ml. The collagen gel lattice was prepared by mixing 1 part of cell suspension with 4 parts of ice-cold 3 mg/ml collagen gel solution. A volume of 0.5 ml of the cell-collagen mixture was added to each well of a 24 well plate and incubated for 1 hr at 37°C in 5% CO_2. After collagen polymerization, 1 ml of HUVEC medium was added drop wise to each collagen gel lattice. After two days, stress had developed in the collagen matrix. Therefore at this point, to initiate cell contraction, the attached collagen

gels were gently released from the sides of the culture dishes with a sterile pipette tip. The degree of cell contraction was evaluated by measuring the diameter of the free-floating collagen gels after 5 days.

14   Immunofluorescence

F-actin and vinculin

For staining subconfluent HUVEC, two days after siRNA transfection, cells were harvested and seeded at 20,000 cells/coverslip on coverslips coated in gelatin (0.1% (w/v) in PBS) and incubated for 4 hours at 37°C with 5% CO_2 in complete medium before washing and fixing.   In order to fluorescently stain proteins during wound healing, two days after siRNA transfection, 5 x 10^4 cells were seeded onto 13 mm gelatin-coated glass coverslips (VWR, Canada) in 24-well plates. The following day, the cells were wounded by scraping across the surface with 2 μL sterile pipette tips and washed once with PBS. Fresh media was added and the wounds were allowed to heal for 6 hours in 5% CO_2 at 37°C before fixing.

Prior to fixing, cells were gently washed with PBS. They were then fixed with 4% (w/v) paraformaldehye (PFA) in PBS for 15 minutes. The cells were washed again before permeabilizing with 0.1% (v/v) triton-X-100 in PBS for 4 minutes. The cells were blocked in IF blocking buffer (3% (w/v) BSA, 10% (v/v) FCS, 0.1% (v/v) tween-20, 0.01 % (w/v) sodium azide in PBS) for one hour at room temperature. The cells were then incubated for one hour at room temperature in 20 μg/ml anti-vinculin antibody (mouse monoclonal, Sigma) diluted in IF blocking buffer. Cells were washed with PBS then incubated with phalloidin-TRITC (50 μg/ml, Invitrogen) and 4 μg/mL anti-mouse immunoglobulin Alexa-fluor 488 (Invitrogen) for 30

minutes at room temperature in IF blocking buffer. Coverslips were mounted using ProLong Gold Antifade reagent with DAPI (Invitrogen).

For visualization of f-actin and focal adhesions in GFP and GFP-daRhoJ lentivirally transduced cells were performed as described above, except that the secondary antibody used to stain vinculin was 4 µg/mL anti-mouse immunoglobulin conjugated to Alexa-fluor 546 (Invitrogen). For these cells separate slides were used for vinculin and f-actin staining.

Immunofluorescence of endogenous RhoJ

For staining endogenous RhoJ, HUVECs were cultured on glass coverslips coated with 0.1 % (w/v) gelatin/PBS for 16 hrs (o/n). Cells were fixed and permeabilized with ice cold methanol for 5 min and blocked in 4 % (w/v) BSA/PBS for 1 hr at room temperature. Coverslips were incubated with primary antibodies diluted in 4 % (w/v) BSA/PBS for two hours at room temperature: anti-RhoJ (rabbit polyclonal antibody, generated as described below) in combination with anti-vinculin (mouse monoclonal, Sigma) or anti-pFAK Y397 (mouse monoclonal, BD Transduction Laboratories). Coverslips were washed 2 x 5 min in PBST and was then incubated with secondary antibody [anti-mouse Alexa-fluor 546 and anti-rabbit Alexa-fluor 488 (Invitrogen)] diluted in 4 % (w/v) BSA/PBS for 45 min. Cells were washed 3 x 5 min in PBST and finally in water. Cells were mounted in ProLong Gold antifade reagent - mounting medium with DAPI (Invitrogen).

All immunofluorescence was analysed using the Axiovert 100M confocal microscope and LSM 510 software (Zeiss). LSM 510 software was used to calculate mean fluorescent instensity of a

particular channel using the following equation: mean intensity = sum of (number of positive pixels x intensity levels)/number of positive pixels. Focal adhesions were manually counted using the cell-counter plugin tool of ImageJ to count the areas of vinculin staining in each cell.

15   Riboprobe synthesis for *in situ* hybridization

Riboprobes were synthesized from plasmids pGEM3Z-mRhoJ (mouse RhoJ 1-645 of coding region), pGEM3Z-mVWF (7838-8387 of coding region) and pGEM3Z-hRhoJ (human RhoJ 1-645 of coding region). Plasmid DNA was linearized to generate templates for sense and antisense probe generation. The linearized DNA was then purified from the enzymatic reaction with QIAquick PCR purification kit (Qiagen) according to the manufacturer's instructions. 1 µg of linearized DNA was transcribed and labelled with the DIG labelling kit (Roche Applied Science), then the probe was purified using mini quick spin columns (Roche Applied Science).

16   Mouse embryo whole-mount *in situ* hybridization

Mouse embryos were collected from matings of C57BL/6 mice at embryonic day (E) E9.5. Embryos were staged by assigning noon of the day that a vaginal plug is found as E0.5. The matings were set up and mice were culled at E9.5 by the Biomedical Services Unit at the University of Birmingham. The embryos were dissected out by removing the uterus from the mother, trimming the mesometrium. The decidual swelling was then removed from the uterus and placed in ice cold PBS. The embryos were carefully removed from the deciduas before removing the thin Deichert's membrane from the embryos. The embryos were immediately transferred to freshly prepared 4% (w/v) PFA in DEPC-treated PBS at 4°C overnight whilst gently rocking. The embryos were then washed with DEPC-treated PBS before being dehydrated

through sequential 5 minute incubations at room temperature in 1 ml 25% (v/v), 50% (v/v), 75% (v/v) and then 100% methanol in 0.1% (v/v) tween-20 DEPC-treated PBS (PBST) and stored at -20 °C.

Whole mount *in situ* hybridization protocol was adapted from the protocol described by Piette *et al* [7]. Mouse embryos were rehydrated back through sequential 5 minute incubations at room temperature in 1 ml 75% (v/v), 50% (v/v) and then 25% (v/v) methanol in 0.1% (v/v) tween-20 DEPC-treated PBST and then 5 minutes in PBST with gentle rocking for all incubations.

The embryos were then digested with 10 μg/ml of proteinase K (Sigma) in PBST for 15 minutes at room temperature and washed once with 2 mg/ml glycine (Sigma) in PBST. Embryos were rinsed once with PBST and washed a further 2 x 5 minutes with PBST before being re-fixed in 4% (w/v) PFA / 0.2% (v/v) glutaldehyde in PBS for 20 minutes. The embryos were washed 2 x 5 minutes with PBST and washed once with 50% hybridization buffer [50% (v/v) deionized formamide, 1% (w/v) blocking reagent, 5xSSC, 0.1 mg/ml heparin, 1 mg/ml torula RNA, 0.1% (w/v) CHAPS, adjusted to pH 5.5 with 1 M citric acid] / 50% PBST for 3 minutes. The embryos were then washed once in 100% hybridization buffer for 3 minutes and this was replaced with 400 μl hybridization buffer and the embryos were prehybridized at 65°C for 3 hours. 500 ng of riboprobe was added to 100 μl of hybridization buffer and denatured at 95°C for 5 minutes and then added to the embryos and incubated over night at 65°C. The following day, the riboprobe mix was removed and the embryos were washed in 800 μl of hybridization buffer for 5 minutes at 70°C. Added to this solution was 400 μl of 2 x SSC (Sigma) pH 4.5 which was incubated for 5 minutes at 70°C (this step was repeated 3 times leading to a total volume of 2 ml). The mix was

removed and the embryos were incubated in 2 x SSC pH 7 / 0.1% (w/v) CHAPS (Sigma) for 30 minutes at 70°C. The embryos were then washed with Maleic Acid Buffer – Tween 20 (MABT) [0.1 M Maleic acid, 0.15 M NaCl, pH 7.5 using NaOH] in the following order: 2 x 10 minutes with MABT at room temperature, 2 x 30 minutes MABT at 70 °C, 2 x 10 minutes PBS at room temperature and finally for 5 minutes in PBST.

Embryos were incubated in 1 ml of antibody buffer [10% (v/v) heat inactivated serum, 1% (w/v) blocking reagent (Roche applied science), 1 x PBST] for at least 2 hours whilst rocking gently at 4°C. This was removed and replaced with antibody buffer containing preblocked 1:500 anti-digoxigenin conjugated to alkaline phosphatase antibody (Roche Applied Science) and incubated overnight at 4 °C whilst rocking gently. Embryos were rinsed and then washed 4 x 45 minutes with 4 ml of PBST/0.1% (w/v) BSA (Sigma) at room temperature. Embryos were then washed 2 x 30 minutes in PBST and then 2 x 10 minutes in AP1 buffer [0.1 M NaCl, 0.1 M Tris pH 9.5, 50 mM MgCl$_2$] at room temperature. The AP1 buffer was replaced with 1 ml of BM purple (Roche applied science) and incubated in the dark until a purple signal has developed. The reaction was stopped by washing the embryos 2 x 15 minutes in stop solution [100 mM Tris Ph 7.4, 1 mM EDTA] at room temperature and dehydrated through a methanol series to 100% methanol as detailed above. Embryos were viewed and imaged using Leica MZ16 stereomicroscope and USB 2.0 2M Xli camera (Leica) and stored at 4 °C indefinitely.

17 Fluorescent *in situ* hybridization on human tissue sections

Paraffin embedded tissue sections were obtained from either Cancer Research UK (CRUK) histology service or SuperBiochips Inc. All solutions were DEPC treated. All reagents are from Sigma unless otherwise stated.

Following removal of paraffin with Histoclear (National Diagnostics, UK) for 3 x 5 minutes, the tissues were rehydrated back through sequential 5-minute incubations at room temperature in 100%, 75% (v/v), and then 25% (v/v) ethanol in H_2O. Tissues were then washed for 1 minute in H_2O and 10 minutes in PBS at room temperature. Tissues were re-fixed in 4% (w/v) Paraformaldehyde in PBS for 10 minutes at room temperature. Sections were then washed for 30 minutes with PBS at 37 °C to ensure the right temperature for digestion. The tissue sections were then digested with 0.2% (w/v) Trypsin in PBS for 10 minutes at 37 °C. Following digestion, sections were rinsed once with PBS and then dehydrated through sequential 5 minute incubations at room temperature in 25% (v/v), 75% (v/v) and then 100% ethanol in H_2O. Slides were allowed to air dry for 3 minutes before adding 50 μl of hybridization buffer [50% (v/v) deionized formamide, 2 x SSC, 0.005 M sodium phosphate, 10% (w/v) dextran sulphate, 500 ng digoxigenin labeled riboprobe in nuclease-free H_2O] per slide. Sections were completely covered with RNase-free hybriwells (Invitrogen). The probe was then denatured by heating to 80 °C for 75 seconds using PCR Express Thermal Cycler (Thermo Hybaid) before being incubated overnight at 37 °C. The following day, hyrbiwells were removed and sections were gently rinsed in 2 x SSC with 0.1% (v/v) tween-20. Tissues were then washed in 0.1 x SSC for 30 minutes at 68 °C. Tissues were treated with 0.1 mg/ml RNase A in PBST for 15 minutes at room temperature then rinsed three times with PBST. Sections were blocked in blocking buffer [1/20

FCS in PBST] for 1 hour at room temperature. Tissue sections were then probed with 20 μg/ml

of *Ulex europeaus* agglutinin I (UEAI) conjugated to fluorescein (Vector Labs) and 1 μg/ml anti-

digoxigenin conjugated to rhodamine (Roche) in blocking buffer for 1 hour. Sections were rinsed

three times with PBST and then once with H_2O. Slides were permanently mounted with Anti-

Fade Prolong Gold with DAPI (Invitrogen) and sections were analysed using Axiovert 100M

laser scanning confocal microscope (Zeiss).

18 RNA extraction, cDNA production and qPCR

RNA from HUVEC, HASMC and hPC-PL was extracted using TRI reagent (Sigma) according

to the manufacturer's instructions. cDNA prepared from 2 μg RNA in a volume of 40 μl High-

Capacity cDNA Archive kit (Applied Biosystems, UK) using the random primers according to

the manufacturer's instructions. qPCR for human RhoJ and beta-actin was performed using the

Exiqon probe based system (Roche) as using a Rotor-Gene (Corbett) as previously described [8].

19 Preparing cell lysates

For protein expression analysis from siRNA knockdown experiments and for analysing RhoJ

expression in different cell types, cells were lysed in NP40 lysis buffer as described below. 48 -

72 hours after siRNA transfection approximately 2×10^5 cells were harvested, washed with PBS

and lysed in 30 μl of NP40 lysis buffer [1 % (v/v) NP40, 10 mM Tris pH 7.5, 150 mM NaCl, 1

mM EDTA pH 8, 0.01% (w/v) sodium azide and 1 x protease inhibitor cocktail (Sigma)]. Tubes

were vortexed for 10 seconds and incubated on ice for 30 minutes followed by centrifugation at

20,000 g for 10 minutes at 4°C. Protein concentrations of the lysates were measured by DC

BioRad protein assay kit (BioRad Laboratories). The supernatant was then transferred to a new

tube containing an equal volume of 2x SDS-PAGE sample buffer [100 mM Tris pH 6.8, 10% (w/v) SDS, 20% (v/v) glycerol, 0.2% (w/v) bromophenol blue, 20% (v/v) β-mercaptoethanol] and stored at -20°C. In order to perform western blotting from lentivirally transduced HUVEC or transfected HEK293T cells, cells were lysed in Rho-assay buffer (1 % (v/v) NP40, 1 % (w/v) N-octyl-β-D-glucopyranoside, 25 mM HEPES pH 7.5, 30 mM MgCl2, 150 mM NaCl, protease inhibitors cocktail (Sigma), 10mM NaF, 2mM NaVO$_3$) and processed as described in section 20 below.

20   RhoJ and Cdc42 activation assays

Preparation of GST-PBD beads: GST-PBD was expressed in *E. coli* strain BL21 (DE3) and purified according to standard methods. pGEX KG-PBD was used to produce glutathione S-Transferase – Pak1 p21-binding domain (GST-PBD, the PBD encoded amino acids 1-254 of Rattus norvegicus PAK1 which encompasses the CRIB domain). Briefly, liquid cultures of E. coli were incubated with shaking at 30ºC until they reached the mid-log phase growth, when they were induced with 0.3 mM IPTG for 2.5 hrs. Bacteria were harvested, washed and frozen as a pellet at -80ºC. Subsequently, bacteria were thawed on ice, lysed with ice-cold E. coli lysis buffer (50 mM Tris-HCl, pH 7.5, 50 mM NaCl, 5 mM MgCl$_2$, 1 mM dithiothreitol (DTT) and 1 mM phenylmethylsulfonyl fluoride (PMSF)) and ultra-sonicated for 3 min (Ultrasonicator Vibra CellTM, Sonics & Materials). After sonication Triton X100 was added to final concentration of 1% (v/v) and left on ice for 30 min before centrifugation. Lysates were clarified by centrifugation at 21910 x g for 10 minutes at 4ºC. Then the supernatant was collected and mixed with glycerol to give a final concentration of glycerol 50% (v/v) and stored at -20ºC. Prior to each experiment GST-PBD was bound in batch to glutathione-agarose (Sigma); for each

pulldown, 5 μg of GST-PBD was bound to glutathione-agarose by incubating sufficient bacterial lysate with 12.5 μl of packed beads in *E. coli* lysis buffer in a volume of 125 μl and rotated on wheel for 45 min at 4ºC. They were then washed 3 times with Rho-assay buffer (1 % (v/v) NP40, 1 % (w/v) N-octyl-β-D-glucopyranoside, 25 mM HEPES pH 7.5, 30 mM MgCl2, 150 mM NaCl, protease inhibitors cocktail (Sigma), 10mM NaF, 2mM NaVO$_3$) and finally diluted with this buffer to give 25 % (v/v) slurry. The beads were then ready for the Rho GTPase pull-down assay.

VEGF-A stimulation assay: HUVEC were cultured on gelatin-coated 10 cm plates and starved in M199 medium (supplemented with 4 mM glutamine) for 1 hour. After starving the cells, M199 medium containing 10 ng/ml VEGF-A (Peprotech) was added in a total volume of 5 ml per plate for the specified time period. After treatment medium was quickly removed, the plates placed on ice and 200 μl of Rho-assay lysis buffer was added. Cells were scraped in lysis buffer and incubated in 1.5 ml eppendorf on ice for 10 min. Then lysates were clarified by centrifugation at 21910 g for 5 minutes at 4ºC. 20 μl of each sample lysate was mixed with equal amount of 2x SDS sample-loading buffer (100 mM Tris-Cl, pH 6.8, 20% (v/v) β-mercaptoethanol, 4% (w/v) SDS, 0.2% (w/v) bromophenol blue, 20% (v/v) glycerol) and the remainder was mixed with GST-PBD glutathione agarose beads. Samples were placed on a rotating wheel and the pull-down performed for 45 min at 4ºC. Then the beads were washed 3 times with 1 ml of Rho-assay lysis buffer and resuspended in 30 μl of 2x SDS sample-loading buffer. Finally samples were subjected to the SDS-PAGE and western blotted with RhoJ or Cdc42 specific antibodies, as described below. Densitometry was performed using ImageJ software. For each band, mean grey values were determined, background values subtracted, and the resulting values used to

calculate the amount of activated Rho GTPase relative to total Rho GTPase for each time point. Time point 0 was normalised to 1, and the values for all other time points adjusted accordingly.

21   SDS-polyacrylamide gel electrophoresis and western blotting

Samples were subjected to SDS-PAGE and western blotting using standard techniques. Primary antibodies used were as indicated with horseradish peroxidase (HRP) conjugated secondary antibodies were polyclonal goat anti-mouse immunoglobulins as noted above. The western blots were developed with ECL Western Blotting Detection Reagents (GE Healthcare) or Supersignal (Pierce) and exposed to Hyperfilm MP (Amersham Biosciences).

22   Phospho-myosin light chain assays

HUVEC were either mock transfected or transfected with siControl, RhoJ siRNA D1 or D2 in 6-well plates at a density of 1.5×10^5 using GeneFECTOR™ (Venn Nova, Inc.) according to the manufacturer's recommendations. One day after transfection, 5×10^5 cells were plated on 6 cm plates coated with 600 μl growth factor reduced matrigel (VWR) diluted 1:1 with PBS and cultured in Optimized Medium (TCS CellWorks) for a further 24-48 hours. To harvest cells, plates were placed on ice, the media was removed and 300 μl of 2x Laemmli lysis buffer [80 mM Tris-Cl, pH 7.5, 4% (v/v) β-mercaptoethanol, 2% (w/v) SDS, 10% (v/v) glycerol, 10mM sodium fluoride, 1mM sodium vanadate, 10mM sodium β-glycerophosphate, 0.5mM PMSF and Complete-EDTA free protease (Roche, Diagnostics GmbH)] was added. After scraping, the lysate was transferred to a 1.5 ml tube and immediately snap frozen on dry ice. Lysates were then boiled from frozen for 5 minutes, sonicated for 15s and then centrifuged for 30 minutes at 4ºC. The supernatant was transferred to a new tube, and 225 lysate was added to 75 µl NuPage

LDS load (Invitrogen). This was then subjected to SDS-polyacrylamide gel electrophoresis and western blotting. Membranes were blocked in 5% (w/v) BSA in TBST and then probed with either phospho-MLC2 (thr18/ser19 NEB signalling) or pan-MLC2 (Santa Cruz), followed by an HRP conjugated anti-rabbit immuboglobulin antisera and the ECL Plus detection System (GE Healthcare-Amersham).

23   Development of RhoJ antiserum for immunofluorescence

To make polyclonal anti-RhoJ antibodies, recombinant fusion protein maltose binding protein (MBP)-wtRhoJ was produced and used as the immunogen. Wild type RhoJ without the region encoding the CAAX box (wtRhoJ-CAAX) was cloned into pMAL-2CE. This plasmid was transformed into BL21 (DE3) pLys S *E. coli*, and bacterial extract containing MBP-wtRhoJ-CAAX was prepared according to the protocol described above for GST-PBD. MBP-wtRhoJ-CAAX was purified using amylose beads using standard protocols, and used for immunisations performed by Harlan Sera Lab (Cancer Research UK Central Services, Clare Hall). Rabbits were given 6 injections according to the following schedule. The primary immunisation used 400 μg in complete Freund's adjuvant, and the following 5 injections contained 100 μg of immunogen in incomplete Freund's adjuvant and were given every two weeks thereafter. The rabbits were terminally bled after one week of the 6th injection. The antiserum was purified by first removing the MBP specific antibodies and then purifying RhoJ specific antibodies by incubating with GST-wtRhoJ-CAAX bound to Polyvinylidene fluoride (PVDF) membrane.

To purify a batch of antibody the following was performed in each of six 1.5 ml tubes. Bacterial extract containing 15 μg of MBP protein was incubated with 25 µl packed amylose beads (NEB)

in a final volume of approximately 0.5 ml of *E. coli* washing buffer (50 mM Tris-HCl, pH 7.5, 50 mM NaCl, 5 mM MgCl$_2$) supplemented with 1mM PMSF (Sigma) and rotated on a wheel for 1 hr at 4 °C. The beads were washed 3 times with 1ml of *E. coli* washing buffer and then blocked in 3 % (w/v) bovine serum albumin (BSA)/ tris-buffered saline tween (TBST) for 1 hr at 4 °C. To remove MBP specific antibodies, 0.5 ml of the MBP-RhoJ specific antiserum was then incubated with these beads by rotation on a wheel for 1 hr at 4 °C. The pre-cleared antiserum was collected and the amylose beads washed 4 times with 1 ml of TBST, the pre-cleared antiserum was pooled with the washes and the total volume adjusted to 5 ml with TBST, to give a final total of 30 ml.

10 µg of GST-wtRhoJ-CAAX was loaded in each well of 6 polyacrylamide gels (12%), proteins were transferred to PVDF membranes and stained with Ponceau S dye (Sigma) to identify GST-wtRhoJ-CAAX. The strips of membrane containing GST-wtRhoJ-CAAX were cut out and blocked in 3 % (w/v) BSA/TBST for 1 hr at room temperature. Then each of the 6 membrane strips was incubated separately with 5 ml pre-cleared antiserum over night in the presence of 3 mM NaN$_3$. Membranes were washed 3 x 10 min with TBST, 1 x 10 min with high salt TBST (650 mM NaCl) and 3 x 10 min with TBS. The strips were then combined and bound antibody was eluted in 3 ml of 100 mM glycine (pH 2.5) incubated with the membrane for 7 min on ice rotating. The solution was collected and neutralised with 1 M Tris-Cl (pH 9.5). Then the membrane was subjected to a second elution of the antibody with 3 ml of 100 mM glycine (pH 2.5) and incubated for a further 5 min, collected and neutralised as above. Purified antibodies from each elution were stored separately, and supplemented with 3mM NaN$_3$ and 4 % (w/v)

BSA at 4 °C. The quality of the purified antiserum was checked by western blotting and immunofluorescence using negative control duplex or RhoJ specific siRNA transfected HUVEC.

24   Chemotaxis using the Boyden chamber

Chemotaxis was assayed using a 48-well modified Boyden chamber (Neuro Probe, USA) with 8 μm pore size polycarbonate nucleopore filters (Neuro Probe, USA). Filters were coated with gelatin (0.1% (w/v) in PBS) and placed over a lower chamber containing 30 μl per well of complete HUVEC media as the chemoattractant factor. Cells were incubated in serum-free media for 30 minutes before the assay. Cells were harvested and 2×10^4 cells were seeded per well of the upper chamber in 50 μl basal media of M199 and 4 mM glutamine containing 1% (v/v) fetal bovine serum. After 5 hours incubation at 37°C with 5% CO_2, the filters were removed, fixed in 100% methanol and stained with 100 ng/ml DAPI (Sigma) in PBS for 1 minute at room temperature. The filters were then washed with PBS and placed onto a glass slide and non-migrated cells were wiped away with a wet cotton swab. Cells that migrated through the pores towards the chemoattractant were viewed using Axiovert 100M confocal microscope and LSM 510 software (Zeiss). The sum of migrated cells in five random areas for each well was calculated for at least 5 replicate wells of each condition.

25   Statistical analyses

All experiments were performed at least 3 times with similar results. Data is plotted with error bars representing standard error of the mean. In order to test for statistical differences in the data, the Kruskal-Wallis test was used, in order to compare defined pairs of groups, the Mann-Witney test was performed, except for the scratch wound and gel contraction assays where the

Student T test was used. Statistical significance is denoted as follows: *** p<0.001, ** p= 0.001 to 0.01 and * p=0.01 to 0.05. To analyse VEGF mediated activation of RhoJ and Cdc42 the Wilcoxon signed-rank test was used to compare data from each timepoint with time zero which was normalized to 1. All calculations were performed using the Prism software (GraphPad).

26   References

1.   Maciag T, Cerundolo J, Ilsley S, Kelley PR, Forand R. An endothelial cell growth factor from bovine hypothalamus: identification and partial characterization. *Proc Natl Acad Sci U S A.* 1979;76:5674-5678.

2.   Ades EW, Candal FJ, Swerlick RA, George VG, Summers S, Bosse DC, Lawley TJ. HMEC-1: establishment of an immortalized human microvascular endothelial cell line. *J Invest Dermatol.* 1992;99:683-690.

3.   Abraham S, Yeo M, Montero-Balaguer M, Paterson H, Dejana E, Marshall CJ, Mavria G. VE-Cadherin-mediated cell-cell interaction suppresses sprouting via signaling to MLC2 phosphorylation. *Curr Biol.* 2009;19:668-674.

4.   Mavria G, Vercoulen Y, Yeo M, Paterson H, Karasarides M, Marais R, Bird D, Marshall CJ. ERK-MAPK signaling opposes Rho-kinase to promote endothelial cell survival and sprouting during angiogenesis. *Cancer Cell.* 2006;9:33-44.

5.   Bell E, Ivarsson B, Merrill C. Production of a tissue-like structure by contraction of collagen lattices by human fibroblasts of different proliferative potential in vitro. *Proc Natl Acad Sci U S A.* 1979;76:1274-1278.

6.   Vernon RB, Sage EH. Contraction of fibrillar type I collagen by endothelial cells: a study in vitro. *J Cell Biochem.* 1996;60:185-197.

7.   Piette D, Hendrickx M, Willems E, Kemp CR, Leyns L. An optimized procedure for whole-mount in situ hybridization on mouse embryos and embryoid bodies. *Nat Protoc.* 2008;3:1194-1201.

8.   Herbert JM, Stekel D, Sanderson S, Heath VL, Bicknell R. A novel method of differential gene expression analysis using multiple cDNA libraries applied to the identification of tumour endothelial genes. *BMC Genomics.* 2008;9:153.